mathematics

MDPI

Review

Mechanical Behavior Analysis-Based Finite Element Method of Composites: A Review

Maria Luminita Scutaru [1], Pop Nicolae [2,*], Sorin Vlase [1,2], Ana Maria Mitu [2,*], Tudor Sireteanu [2] and Violeta Mihaela Munteanu [1]

[1] Department of Mechanical Engineering, Transilvania University of Brasov, 500036 Brasov, Romania; lscutaru@unitbv.ro (M.L.S.); svlase@unitbv.ro (S.V.); v.munteanu@unitbv.ro (V.M.M.)
[2] Institute of Solid Mechanics of the Romanian Academy, Str. C. Mille, 15, 010141 Bucharest, Romania; tudor.sireteanu@imsar.ro
* Correspondence: nicpop@imsar.ro (P.N.); ana.maria.mitu@imsar.ro (A.M.M.)

Abstract

The mechanical behavior of a composite is determined by the value of the engineering constants for the composite under consideration. If we study a homogeneous and isotropic composite, then two engineering elastic constants are needed to characterize the material; if we refer to a transversely isotropic composite, five elastic constants are needed. For more complex materials it can be necessary to determine more elastic constants in order to obtain the behavior of the composite in practical applications. In this paper, the authors present the main classic methods for calculating the engineering constants of a fiber composite material that are used in parallel with the finite element method (FEM) and highlight the advantages (and disadvantages) of using direct FEM to achieve this. The arrangement of identical fibers provides regularities that allow for easier calculations and, in some cases, the application of simple methods. The results that have already become classics, current results, and unusual examples are all critically presented in this study. All of these findings are discussed in relation to the use of the FEM, either as the primary calculation method or as a useful aid in the application of classical methods. The paper focuses on presenting research on the use of FEM for this purpose. For the different approaches discussed and for the area overall, future research directions are emphasized.

Keywords: engineering constants; elastic parameters; fiber; matrix; classical models; two-phase composites; finite element method; composite design

MSC: 65N30; 65N22; 65K15

Check for updates

Academic Editor: Lihua Wang

Received: 28 March 2026
Revised: 7 June 2026
Accepted: 17 June 2026
Published: 23 June 2026

Copyright: © 2026 by the authors. Licensee MDPI, Basel, Switzerland. This article is an open access article distributed under the terms and conditions of the Creative Commons Attribution (CC BY) license.

1. Introduction

Composite materials are currently used in important industrial sectors such as aeronautics, automotive, naval and energy. Composites offer major advantages due to their high strength-to-weight ratio, the ability to tailor mechanical properties and their low manufacturing cost. A great number of factors, including material complexity, ambient circumstances, modeling and testing difficulties, scale effects, and the requirement for interdisciplinary approaches for specific applications, must be considered when determining the elastic constants of fiber-reinforced composites. These constants determine the mechanical behavior of the material and define the properties chosen for a specific application. The necessity of modeling real-world settings (high temperatures, humidity levels, and various loading scenarios) and the very diverse and frequently contradicting properties of the

fibers and matrix materials are the causes of all these issues. To increase the accuracy of calculus methods to determine the mechanical characteristics and in-service behavior of these materials, a comprehensive approach that addresses all these issues calls for both sophisticated modeling tools and modern experimental methodologies.

The study of the mechanical behavior of composite materials is an area that is continuously developing, given the current advances in the sector. The modern period is characterized by an explosive dynamic of practical applications, which also involves the strong advancement of production methods, modeling approaches, and the desire to increase the characteristics of the materials used. The literature on techniques for determining composite materials' elastic constants is extensive. To show how these techniques developed concurrently with the application of FEM, we shall highlight a few of these studies.

Thus, the emergence of composites led to the first studies that attempted to use the regularity that appears in these materials to determine upper and lower bounds for elastic constants. It should be mentioned that not all five of the effective models required for the transversally isotropic composite's characterization can be created with Hill's [1,2] and Hashin's [3–8] pioneering theories. In these models it is considered that the two phases of the composite are thought to be isotropic. Remember that when determining the previously indicated limits, the concentration of the two phases is considered, not the form of the reinforcing phase. Therefore, it makes sense to suppose that these borders may occasionally vary considerably. We mention that the results are usually far from the experimentally determined values. This happens when the regular arrangement is far from the real situation, when there are big differences between a regular array and a real one.

The studies carried out aimed at determining the calculation methods for different composites used gradually in the industry. For example, a model for the modeling of an aramid fiber composite is described in [9–11], a study to determine a lower bound of longitudinal elastic modulus for a three-phase fibrous composite is developed in [12], and the analysis of an application made of Kevlar is presented in [13]. Different models and calculation methods are presented in [14–18]. The study of natural fibers and textiles is presented in [19–22]. Other aspects related to the specific problem are dealt with in [23–27]. Basics of the study and elastic constants can be found in a rich literature such as [28–32].

It goes without saying that the production of nanofibers and nanomaterials (such as graphene and carbon nanotubes) has led to their use as fillers and provided materials with better mechanical qualities [33,34]. The emergence of hybrid composites represents another relatively recent trend. So, by combining different fibers with different properties (glass, carbon, aramid and so on) within the same composite, it is possible to obtain a composite with improved properties by leveraging the particular properties offered by each type of fiber. It is possible to improve the load transfer, the stability at different temperatures and, as a consequence, a better mechanical behavior [35,36]. Multi-scale modeling that bridges the gap between macro-scale (entire composite structure) and micro-scale (fiber and matrix) behaviors is probably going to be the main focus of future research [37,38].

A thorough understanding of the mechanical characteristics of composite materials is necessary for applications in the field of artificial intelligence [39,40]. Machine learning (ML) techniques can significantly increase the accuracy of creep behavior predictions in composite materials by spotting complex patterns and nonlinear correlations in data that traditional models would miss. In practical applications, creep in composites is influenced by a wide range of parameters, including matrix and fiber properties, temperature, stress levels, fiber orientation, time, and environmental conditions. The simplifications employed in a typical model might not reflect certain interactions. By using machine learning (ML) tools like neural networks and decision trees, more complex models (nonlinear, multi-

dimensional) can be produced. This method has been used in a number of papers devoted to innovative research applications [41–45].

To take into consideration the intricate development of damage, such as delamination, matrix cracking, and deterioration of the fiber-matrix interface, integrated damage mechanics are being incorporated into predictive models. These models would yield more accurate lifetime and failure estimates by taking material degradation over time into account [42–44].

Predictive models are incorporating integrated damage mechanics to account for the complex evolution of damage, including delamination, matrix cracking, and deterioration of the fiber-matrix interface. By accounting for material degradation over time, these models would produce lifetime and failure estimates that are more accurate [42–44].

It is crucial to test composites in a lab to see how well the suggested or used models match the actual behavior of the materials. Because of this, there are a lot of publications and suggestions for methods that should be used when conducting the tests [44–48].

Composite materials are used in a variety of settings and circumstances in engineering applications. Understanding how fiber-reinforced composites react to various environmental conditions, such as temperature, humidity, UV rays, and thermal cycles, is therefore essential. Nowadays, composites are used in a variety of industries, including building, infrastructure, medical technology, automotive, and aerospace. To cover the vast array of composite applications, it is also essential to know the mechanical properties [49–57].

It is necessary to combine a number of disciplines, including environmental science, mechanical engineering, materials science, and computational modeling. Governmental, business, and academic entities must work together. New standards, testing procedures, and modeling approaches that provide more accurate forecasts may result from this [58,59].

In order to save time when designing and developing a new product, accelerated testing techniques are being used more and more. Through more effective experimental data collection and analysis, robotics and advanced automation are being employed more and more to conduct experiments on a large number of specimens [60,61].

The key challenges and issues faced in the investigation of the mechanical characteristics and behavior of fiber-reinforced composite materials are revealed by the examination of the primary findings thus far. The basic notations of our paper are presented in Appendix A. The following is a list of some of the challenges faced by researchers in the literature that was presented:

- The significant heterogeneity of composite materials, where the phases (fibers and matrix) have highly varied mechanical and physical properties, complicated interactions, and time-varying parameters, necessitates complex constitutive models. Composites can have a non-uniform material distribution, non-linear material properties, and both plastic and elastic deformation over time. In order to have a precise creep forecast, anisotropic and viscoelastic/viscoplastic models must be used.
- A key factor in mechanical behavior is interfacial behavior. A weak or poorly bonded surface can cause delamination or microcracking, which significantly affects mechanical performance. The type and quality of these contacts can have a significant impact on the stress transmission between fibers and matrix.
- It is challenging to understand and model scale effects, or how microstructural events affect macroscopic behavior. The size, shape, and lay-up arrangement of the composite material can have a significant impact on the mechanical models, and it is often difficult to generalize these effects across a wide range of composite systems.
- Environmental factors can sometimes become important in specific circumstances. Over time, moisture, UV light, or harsh chemicals that damage the matrix or break down the fibers can change the creep behavior of fiber-reinforced composites. In practical applications, composite sites may encounter both continuous loading (creep)

and cyclic loading (fatigue) at the same time. In this way, the picture that is displayed to us is complex and demands careful study and modeling.

- Prediction models, which incorporate other elements, such as material properties, loading conditions, and environmental characteristics, into a single model, require extensive experimental data and advanced computational approaches.

In conclusion, examining mechanical behavior in fiber-reinforced composites requires addressing complex issues related to testing challenges, material heterogeneity, temperature sensitivity, interfacial features, and damage evolution. To address these problems, a combination of experimental, computational, and theoretical approaches is required. For composites to be designed and used in a range of industries, especially those where materials are subjected to constant loads over time, it is essential to comprehend their mechanical behavior. Future research on the behavior of composites is likely to be impacted by advancements in material science, environmental conditions, testing protocols, and computational techniques. The paper aims to present the main modeling methods and methods for obtaining mechanical characteristics for composites that use polymers as matrices. The results can be extended, with some precautions, to ceramic materials or metals. We have introduced a table with the advantages and disadvantages of the classic methods of the calculus of elastic constants (Table 1).

Table 1. The advantages and disadvantages of the classical methods.

Method	Advantages	Disadvantages
Homogenization	1. Reduction in modeling complexity. Allows the replacement of the complex microstructure with an equivalent material characterized by effective elastic constants (Young's modulus, shear modulus, Poisson's ratio, etc.). 2. Saving time and computational resources Homogenization significantly reduces the size of the problem and the computational time. 3. Estimation of properties before manufacturing, without the need to manufacture and test a large number of samples. 4. Establishes the connection between microstructure and macroscopic behavior and allows studying the influence of fiber volume, fiber orientation, inclusion shape, and phase distribution on the global elastic properties of the composite. 5. Possibility of material optimization. 6. Has good applicability for anisotropic materials. 7. Easy integration into structural analyses. Thus, the homogenized elastic constants can be directly introduced into structural calculation programs and numerical simulations at a macroscopic scale. 8. Reduced experimental costs due to the number of mechanical tests required for material characterization that can be reduced.	1. Loss of local information (local distributions of stresses and strains are no longer explicitly described). Stress concentrations around fibers, pores or defects cannot be identified. Local phenomena that can initiate damage are ignored. 2. Dependence on model assumptions. Different models can lead to different values of elastic constants. 3. Insufficient representation of the real microstructure. In reality there are agglomerations of fibers, voids, misalignments, manufacturing imperfections that can significantly modify the effective stiffness. 4. Limitations for materials with nonlinear behavior. 5. Difficulties with materials with high property contrast. 6. Sensitivity to the choice of representative volume (RVE). If the RVE is too small, the calculated properties are not representative; if it is too large, the computational cost increases considerably. 7. Inability to describe scale effects. 8. Incomplete estimation of damage phenomena.

Table 1. *Cont.*

Method	Advantages	Disadvantages
Variational methods	1. Provides upper and lower bounds on the effective properties. These bounds provide a range within which the real properties of the composite should lie. 2. Can handle complex microstructures. Can be applied to composites with fibers, laminated materials, porous materials, and materials with randomly distributed inclusions. 3. Rigorous mathematical foundation. 4. Computational efficiency. 5. Natural integration with the finite element method.	1. Results depend on the chosen approximation functions. An inappropriate choice can lead to poor estimates. 2. Usually provides bounds, not the exact solution. If the range is wide, practical utility decreases. 3. Difficulties for very inhomogeneous microstructures. 4. Sophisticated mathematical implementation. 5. Sensitivity to homogenization assumptions.
Mori–Tanaka	1. Good accuracy for moderate volumes of reinforcement (with small and medium volume fractions of inclusions, especially when they are relatively uniformly distributed). 2. Low computational cost. 3. Includes the effect of the shape of inclusions. Can consider long fibers, short fibers, spherical particles, and ellipsoidal inclusions. 4. Provides anisotropic properties. 5. Solid theoretical basis.	1. Reduced accuracy at high volume fractions. 2. Uniform distribution assumption. 3. Limitations for very large stiffness contrasts. 4. Imperfect representation of interactions between inclusions. 5. Less suitable for damaged materials. 6. Need for Eshelby tensor.
FEM	1. Allows modeling of complex geometry (non-uniformly distributed fibers, different orientations of reinforcement, porosities and defects). 2. Determines effective properties for heterogeneous materials (effective Young's modulus, Poisson's ratios, shear moduli, full stiffness matrix). This is useful for laminated composites, textiles or with three-dimensional architectures. 3. Reduces the need for experimental tests. 4. Allows rapid parametric studies. The influences of fiber volume, inclusion shape, matrix properties, and reinforcement orientation can be investigated. 5. Provides detailed local information (stress distributions, stress concentrations at interfaces, areas susceptible to damage). 6. Applicability for anisotropic materials.	1. High computational cost. This aspect becomes critical for complex 3D models. 2. Dependence on the quality of discretization. 3. Requires accurate data on constituents. 4. Sensitivity to boundary conditions. 5. Complexity in modeling and validation. Building a correct FEM model requires experience in composite mechanics, knowledge of homogenization, convergence verification, and experimental validation. 6. Results are approximate.

By offering the latest approaches to the use of FEM, alone or in combination with other recognized methods, the work completes the reviews conducted over the course of five decades of research on composite materials. As a result, it can offer a more thorough and current perspective on the calculation models.

2. Models and Methods to Determine the Elastic Coefficients

The very large range of combinations of materials, concentrations, microstructures available for the composition of a composite material demands a series of experimental analyses to determine the mechanical properties of the different combinations, almost impossible to perform due to the costs that this would impose. As a result, the problem of

estimating these properties by calculation arises, i.e., the composition of suitable mechanical models, which will then be validated by experience, allowing the treatment of a large number of combinations, similar in certain respects, but composed of different materials, with different dimensions, etc. The main models used in research will be presented below, in parallel with the use of FEM to solve them.

2.1. Micromechanical Models

2.1.1. General Considerations

A basic method for calculating the elastic constants of composites is micromechanical analysis. The method uses information about its structure at the microscopic level. In this way, it is possible to consider the mechanical interactions between the fiber and the matrix and, based on the knowledge of the composite geometry at the micro level and the mechanical properties of the constituent phases, to obtain the properties of the composite material at the macromechanical scale. To perform this analysis, it is necessary to know the microstructure (component shape, material, geometry, size, orientation, distribution, etc.), stress–strain relationships, stiffness, and fracture mechanisms. In this way, relationships can be obtained that satisfactorily predict the general physical properties (modulus of elasticity, strength, thermal conductivity).

Based on the results obtained, assessments can then be made on the behavior of the material, such as understanding the initiation of damage (cracking), optimizing the microstructure design (fiber volume fraction, geometry, alignment, etc.) and determining behavior under different loading conditions [62–65].

2.1.2. Model

The properties of the various components, including the fiber and matrix, as well as their interactions, determine the composite's overall traits. The fibers in a unidirectional composite are actually dispersed at random throughout the matrix. Nevertheless, it seems sensible to take into account some regularity in the fiber dispersion. There are many models for different fiber configurations. For our purposes, we provide a common model that may be used to develop more complex layouts. This model is made simpler by its symmetry and periodicity. The square array in Figure 1 illustrates this circumstance.

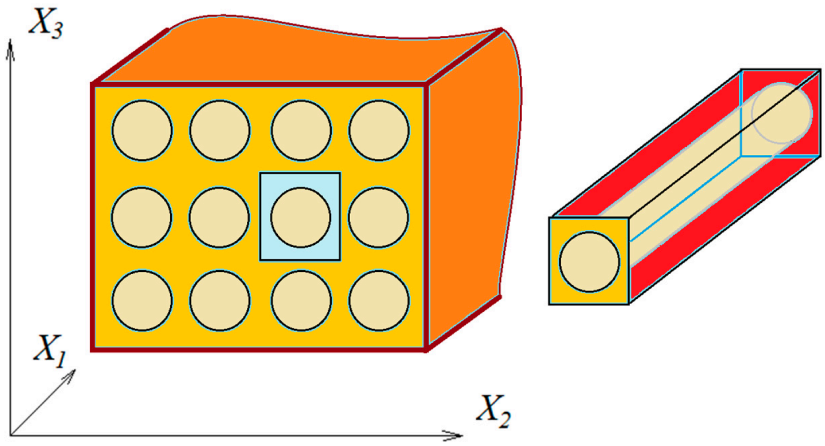

Figure 1. Square fiber packing geometry of a unidirectional composite.

The following presumptions apply to composites reinforced with fibers studied:

- A rectangular array of fibers that are enlarged in the X_1 direction defines the X_2–X_3 plane. Our presentation indicates that the fibers are linearly elastic and anisotropic,

while the polymeric matrix is nonlinearly viscoelastic but isotropic. In fact, when dealing with nonlinear material, these assumptions might be altered;

- Since there is just a mechanical connection between the fibers and matrix, no cracks or holes may occur under strain;
- The previously described regular and periodic packing reduces the problem's size and complexity, allowing for the examination of a representative cell. Note that Figure 2 shows one of the recurrent units of the periodical pattern shown in Figure 2a. It is believed that the fiber has a circular cross-section. The representative unit cell (RUC) (also known as the representative volume element, or RVE) can thus be composed of two subcells, each of which represents a quarter of a fiber and the associated matrix material, as shown in Figure 2b. Furthermore, the unit cells are believed to be small in comparison to the overall size of the composite.
- The analytical theory of RVEs is presented in [66].

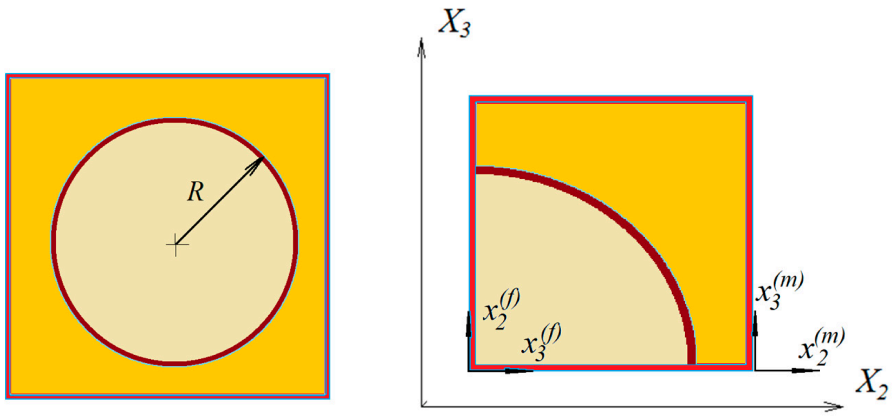

Figure 2. The repeating cell of a square fiber array (**a**) and the representative unit cell (RUC) with the local coordinates (**b**).

A local reference frame (X_1, $x_2^{(\lambda)}$, $x_3^{(\lambda)}$) is introduced for each subcell in the typical cell, with its origin situated as indicated in Figure 2. Both fiber ($\lambda = f$) and matrix () constituents are symbolically represented by the letter "λ". Additionally, a first-order linear expansion is used to represent the displacement in each of the two subcells as a function of the distance between the local coordinate axes and the origin [67,68]. Accordingly, the displacement at any given location within the subcell is as follows:

$$u_i^{(\lambda)} = u_i^{o(\lambda)} + x_2^{(\lambda)}\xi_i^{(\lambda)} + x_3^{(\lambda)}\zeta_i^{(\lambda)} \; ; \; i = 1,\ 2,\ 3 \ . \tag{1}$$

Along the x_i axis, it is noted with u_i^o the component i of the displacement of the local reference frame's origin. The sizes $\xi_i^{(\lambda)}$ and $\zeta_i^{(\lambda)}$, respectively, are the coefficients showing the linear dependence on $x_2^{(\lambda)}$ and $x_3^{(\lambda)}$. Establishing the relationship between the composite's average stresses and average strains is the presentation's main goal. The coefficient of the overall constitutive law will be provided by these relations. Anisotropic bodies' strain-displacement relations result in the following:

$$\varepsilon_{ij}^{(\lambda)} = \frac{1}{2}\left(\frac{\partial u_i^{(\lambda)}}{\partial x_j} + \frac{\partial u_j^{(\lambda)}}{\partial x_i}\right) \; ; \; i, j = 1,\ 2,\ 3. \tag{2}$$

When $i \neq j$ it can be used in the notation: $\gamma_{ij}^{(\lambda)} = 2\varepsilon_{ij}^{(\lambda)}; i, j = 1, 2, 3\ ;\ i \neq j$ for the engineering shear strain. Substituting Equation (1) into Equation (2) it obtains:

$$\begin{gathered} \varepsilon_{11}^{(\lambda)} = \frac{\partial u_i^{o(\lambda)}}{\partial X_1}; \varepsilon_{22}^{(\lambda)} = \xi_2^{(\lambda)}; \varepsilon_{33}^{(\lambda)} = \zeta_3^{(\lambda)}; \\ \gamma_{23}^{(\lambda)} = \left[\xi_3^{(\lambda)} + \zeta_2^{(\lambda)}\right]; \gamma_{31}^{(\lambda)} = \left[\frac{\partial u_3^{o(\lambda)}}{\partial X_1} + \zeta_1^{(\lambda)}\right]; \\ \gamma_{12}^{(\lambda)} = \left[\frac{\partial u_2^{o(\lambda)}}{\partial X_1} + \xi_1^{(\lambda)}\right]. \end{gathered} \tag{3}$$

The following stages are required in order to achieve the general behavior of the composite.

Finding the stresses that each subcell experiences from an externally applied continuous load is the first step. Providing continuity of tractions along the phase interfaces is essential. The strains in the representative cell must next be determined using the induced strains in each subcell. It is crucial to keep in mind that all stresses and strains are evaluated on an average basis. For the composite to be regarded as continuous, all displacements must be continuous between neighboring cells and across the subcell boundaries of the unit cell.

Finally, the Hooke law relation to the previously obtained average stresses and strains will be taken into consideration while determining the constitutive law [69–73].

2.1.3. Applications and Future Developments

A unidirectional composite subjected to longitudinal and/or transverse normal loading can be modeled using the micromechanics process. The mathematics of stresses and strains continues to be the primary issue. To assist in determining these values, finite element software is typically used. The micromechanical models incorporate the constitutive material properties, which vary with temperature and time. For example, to study the nonlinear viscoelastic behavior, Schapery's nonlinear constitutive equation [74] for isothermal uniaxial loading conditions. The corresponding stress from the matrix is taken into account for the triaxial stress state that results from uniaxial loading in the composite, making all viscoelastic parameters reliant on a single invariant. The constitutive equation was significantly reduced when it was discovered that Poisson's ratio was either an extremely weak function of time or nearly independent of it. In [74], micromechanical models are thoroughly examined.

FEM is extensively used in the literature, recently, for building mixed models for the analysis of composites. Within a micromechanical model, FEM is used to determine the stress and strain field. The impact of a metal-matrix long-fiber composite's fiber-matrix interface is examined using a micromechanical model created using the FEM [75]. Based on a cohesive zone model, if a bilinear law exists, cohesive elements are used to study the fiber-matrix interaction. Another simple micromechanical model is proposed to estimate the macroscopic mechanical properties of continuous bidirectional fiber-reinforced composites (CBFRC) [76]. In this model, the Poisson effect is ignored. For the success of the model, the FEM approach is used. Results are obtained that can be expressed as a function of the fiber volume fraction (obviously also of the material properties). A precise and simple micromodel that may be used with a code of finite, explicit elements based on DYNA3D is used to simulate the behavior of structural components under various conditions, such as the impact of collision [77]. The implemented model is validated using a few examples, such as the graphite/epoxide tubular subimpact axial structure.

For the study of a metal-ceramic bimaterial, a finite element analysis was performed on a micromechanical model [78]. A wide range of applications can be found in the literature [79–85].

We identify the development directions in the micromechanical analysis of the fiber-reinforced composite materials, which are based on the previously presented literature and on the use of FEM to determine the field of strain and stress:

- Various physical circumstances. For instance, it is possible to combine environmental, mechanical, and thermal influences;
- Time-dependent interface behavior models must take into account the complexity of engineering systems;
- Additionally, microstructural variability must be taken into account;
- Currently, research in all engineering domains consistently uses multiscale techniques to study systems;
- Information that aids in the creation of more precise models or yields results more quickly can be obtained by using the particular characteristics and usage circumstances of a material;
- The application of machine learning is beginning to gain traction in the field, as it does in all other fields. To speed up property predictions, machine learning algorithms can be combined with micromechanical simulations. Alternatively, physics-informed neural networks (PINNs) can be used to incorporate constitutive creep laws into ML models with physical constraints, or surrogate models trained on high-fidelity micromechanical simulations can be used to explore large design spaces.

2.1.4. Use of FEM in the Development of the Method

The use of anisotropic elasticity in determining the mechanical constants of composite materials is essential because composites do not behave identically in all directions. Their properties depend on the orientation of the fibers, the layered structure and the type of matrix. In the case of fiber-reinforced composites, the stiffness and strength are much higher in the fiber direction than transversely. For such materials, Hooke's law takes the general form and requires more elastic constants than in the case of isotropic materials. For example, for an orthotropic material (a common case in laminated composites) the following are required: 3 Young's moduli: E_x, E_y, and E_z; 3 shear moduli: G_{xy}, G_{yz}, and G_{xz}; and 6 Poisson's ratios. A description of the material in terms of anisotropic behavior allows a realistic description of the behavior of the composite, offers the possibility of more precise determination of mechanical constants and allows for separate evaluation of properties in the direction of the fibers, the design of aerospace structures, wind blades, automobiles or in civil engineering. Such anisotropic analysis helps to choose the optimal orientation of the layers, with a reduction in mass in parallel with an increase in the stiffness and strength of the material. Classical analysis methods cannot generally satisfy all the requirements related to design and calculation and as a result methods and models have been introduced to help in performing dynamic analysis. FEM represents a substantial aid for the success of such an analysis, based on classical, standard models, due to the special capabilities and versatility of the method.

Obviously, the method also presents disadvantages identified by researchers such as high mathematical complexity (determined by the existence, in the general case, of 21 independent elastic constants). The experimental verifications that are required involve high costs and time required (finally materialized also in costs). The results depend significantly on the accuracy of the information introduced into the models, and the real orientation of the fibers, porosity, lamination defects or inherent local variations must be considered. Interactions are generally difficult to physically separate and there is also a difficulty in the physical interpretation of the models and the results obtained. Consequently, methods based on anisotropic elasticity require more input data, consume more calculation time, and may have convergence problems. They provide a much more

accurate description of the mechanical behavior of composite materials and allow the precise determination of the elastic constants relevant for design and simulation but come with the disadvantages listed above.

2.2. Analytical Methods

2.2.1. Estimation of Bounds: Models and Methods

Among the most popular methods are variational approaches that give upper and lower bounds on the modulus of elasticity or other elastic constants (such as bulk modulus, shear modulus, Poisson's ratio, etc.). The accuracy of the estimates using this method is indicated by the difference between the two limits. They are generated for specific kinds of boundary conditions and are usually somewhat imprecise. In the presentation we exemplify the method for the elastic constants for a polymeric material reinforced with rectangular patterned parallel cylindrical fibers.

The literature offers a variety of techniques for forecasting the constants of the elastic/viscoelastic properties of a multi-phase (or two-phase) composite. It is considered that the specimen will be statically homogeneous and transversally isotropic. Predicting the bound on an elastic/viscoelastic property of such a specimen based on its geometrical characteristics and the elastic/viscoelastic moduli of its constituents is the problem to be examined. To demonstrate the difficulties of obtaining the limits on characteristic values of a composite using an analytical technique, let us first suppose that the two components are linear and isotropic. It is assumed that the upper bounds of the bulk and shear moduli are denoted by K_{23}^{+} and G_{23}^{+}, and the lower bounds by K_{23}^{-} and G_{23}^{+}, respectively.

It should be mentioned that in this section and the ones that follow, the "+" and "−" higher indices represent the upper and lower bounds on the characteristic parameters, as in E_{11}^{+}, E_{11}^{-}, ν_{12}^{+}, ν_{12}^{-}. Numerous techniques from the literature can be used to forecast the aforementioned boundaries. By using Hill's theory, one may determine the limits on the bulk modulus K_{23}, the longitudinal Young's modulus E_{11}, and the Poisson's ratio $\nu_1 = \nu_{12} = \nu_{13}$ [86–88]. These bounds are computed using the fiber and matrix volume ratios:

$$K_{23}^{+} = \frac{v_f K_f (K_m + G_m) + v_m K_m \left(K_f + G_f\right)}{v_f \left(K_m + G_f\right) + v_m \left(K_f + G_f\right)}\,; \tag{4}$$

$$K_{23}^{-} = \frac{v_f K_f (K_m + G_m) + v_m K_m \left(K_f + G_m\right)}{v_f (K_m + G_m) + v_m \left(K_f + G_m\right)}\,. \tag{5}$$

where $\lambda = f, m$ (fiber/matrix), the plane-strain bulk modulus K_λ and the shear modulus, respectively G_λ, represent the fiber and matrix phases. Compared to the conventional relations put forward by Voigt (V) and Reuss (R), which are expressed as follows, these bounds were thought to be more striking:

$$K_{23}^{+} = K_V = v_f K_f + v_m K_m\,, \tag{6}$$

$$K_{23}^{-} = K_R = \frac{1}{\frac{v_f}{K_f} + \frac{v_m}{K_m}}\,. \tag{7}$$

for the bulk modulus and

$$G_{23}^{+} = G_V = v_f G_f + v_m G_m \tag{8}$$

$$G_{23}^{-} = G_R = \frac{1}{\frac{v_f}{G_f} + \frac{v_m}{G_m}}\,, \tag{9}$$

for the shear modulus.

For the longitudinal Young's modulus E_{11}, the Hill result is as follows:

$$E_{11}^{+} = E_{1mix} + \frac{4\left(\nu_f - \nu_m\right)^2 v_m v_f}{\frac{v_f}{K_m} + \frac{v_m}{K_f} + \frac{1}{G_f}}; \tag{10}$$

$$E_{11}^{-} = E_{1mix} + \frac{4\left(\nu_f - \nu_m\right)^2 v_m v_f}{\frac{v_f}{K_m} + \frac{v_m}{K_f} + \frac{1}{G_m}}. \tag{11}$$

E_{1mix} is the modulus obtained with the law of mixture, viz.

$$E_{1mix} = v_f E_f + v_m E_m. \tag{12}$$

The bounds on Poisson's ratio can be calculated with the following:

$$\nu_1^{+} = \frac{\nu_{1mix} + \left(\nu_f - \nu_m\right)\left(\frac{1}{K_m} - \frac{1}{K_f}\right) v_m v_f}{\frac{v_f}{K_m} + \frac{v_m}{K_f} + \frac{1}{G_f}}; \tag{13}$$

$$\nu_1^{-} = \frac{\nu_{1mix} + \left(\nu_f - \nu_m\right)\left(\frac{1}{K_m} - \frac{1}{K_f}\right) v_m v_f}{\frac{v_f}{K_m} + \frac{v_m}{K_f} + \frac{1}{G_m}}. \tag{14}$$

It is noted:

$$\nu_{1mix} = v_f \nu_f + v_m \nu_m. \tag{15}$$

Hashin in [89–92] obtained the following formulas for the bulk modulus K_{23}:

$$K_{23}^{+} = K_f + \frac{\nu_m}{\frac{1}{K_m - K_f} + \frac{\nu_f}{K_f + G_f}}; \tag{16}$$

$$K_{23}^{-} = K_m + \frac{\nu_f}{\frac{1}{K_f - K_m} + \frac{\nu_m}{K_m + G_m}}; \tag{17}$$

and for the share modulus G_{23}:

$$G_{23}^{+} = G_f + \frac{\nu_m}{\frac{1}{G_m - G_f} + \frac{\nu_f\left(K_f + 2G_m\right)}{2G_f\left(K_f + G_f\right)}}; \tag{18}$$

$$G_{23}^{-} = G_m + \frac{\nu_f}{\frac{1}{G_f - G_m} + \frac{\nu_m(K_m + 2G_m)}{2G_m(K_m + G_m)}}, \tag{19}$$

The axial shear modulus $G_1 = G_{12} = G_{13}$ can be obtained using the relations:

$$G_1^{+} = G_f + \frac{\nu_m}{\frac{1}{G_m - G_f} + \frac{\nu_f}{2G_f}}; \tag{20}$$

$$G_1^{-} = G_m + \frac{\nu_f}{\frac{1}{G_g - G_m} + \frac{\nu_m}{2G_m}}. \tag{21}$$

The results show that the bounds differ significantly, indicating that this formulation of the limitations cannot be very intriguing from an engineering standpoint.

The study of a composite with isotropic spheroidal inclusions embedded in an isotropic matrix, using the Green's function, is presented in [93]. The results are compared with

experimental results, as well as with the Rosen–Hashin limits. A good agreement between the calculated limits and the experimental data is found. Using additional morphological information in variational models allows obtaining more precise bounds when applying the generalized Hashin–Shtrikman variational principles [94]. The proposed method is applied to a non-linear incompressible, fiber-reinforced, hexagonal periodic elastic composite. At the outset of the theoretical investigation of the values of elastic constants, a number of situations were examined, including examples of composites used in engineering [95–97]. When employing techniques to ascertain the limits of elastic constants, the finite element method also demonstrates its value [98–102].

Analyzing the results obtained using the variational methods for obtaining the lower and upper limits, it is found that there are areas where the difference between the two values that frame the real value is very large. The result obtained is thus very far from the real value. As a result, this method is generally not recommended, except as a first estimate of the limits of the elastic constants.

Estimation of bounds methods are frequently used to evaluate the elastic constants of composite materials when the exact properties are difficult to determine experimentally or numerically. They do not provide a single exact value, but establish a range within which the real mechanical properties of the composite lie. The best known limits are: Voigt limits (uniform deformation), Reuss limits (uniform stress), Hashin–Shtrikman limits and Hill or Mori–Tanaka models.

The advantages of using the estimation of bounds are represented by mathematical simplicity, relatively easy-to-apply methods, fast calculations and easy implementation. It does not use complex numerical models, has a low computational cost, and does not require significant computational resources. With these advantages, they are useful in preliminary estimates at the design phase level of a mechanical assembly that uses composite material. There is no need for detailed knowledge of the geometry or complex simulations. The methods allow a quick comparison of different materials and a preliminary choice of configurations. The disadvantages are limited precision, and the limits obtained can often be too wide for an objective assessment. They do not describe complex microstructures well and have a reduced capacity for local analysis. They are sensitive to the properties of the constituents and present erroneous results for nonlinear behaviors. The finite element method (FEM) offers numerous advantages when used for the calculation or refinement of estimation of bounds methods of elastic constants for composite materials. In this context, FEM not only estimates the limits of mechanical properties but can determine limits closer to the real behavior of the composite by explicitly modeling the microstructure and anisotropic elasticity. FEM allows detailed numerical simulation, the calculation of more realistic limits and the validation of analytical models. The precision is much higher, and the real geometry of the fibers, the orientation, the non-uniform distribution, and the fiber-matrix interface can be modeled. In this way, the limits estimated with classical methods become closer to the real behavior and more restrictive and more useful in engineering. This offers the possibility of modeling the real microstructure. FEM allows the introduction of fibers with discontinuities, porosities, defects, complex inclusions, and 3D textile architectures. With FEM, the influence of volume fraction, fiber orientation, inclusion shape, defects, and interface properties can be analyzed. Although very powerful, the FEM also has limitations such as high computational cost and the need to know more input data.

2.2.2. Applications and Future Developments

Reference [103] provides an example of applying the approach to ascertain a compound's physical characteristics. It is believed that the fibers are uniform. The inner and upper edges are the best estimates offered, while not particularly impressive, according

to a comparison with other approaches, demonstrating the method's utility. In [104], two distinct methods for studying unidirectional composites are introduced. In [105], a three-dimensional finite element model is created to forecast the onset, progression, and fracture toughness of damage in TC33/epoxy unidirectional carbon fiber reinforced polymer (CFRP) laminates under biaxial loading. The expanded Drucker-Prager plastic yielding model is used to define the elasto-plastic behavior of the matrix and the linear elasticity of the carbon fibers. Using a modified version of three-dimensional laminate theory, the out-of-plane modulus of thin QI-CFRP specimens was determined analytically [106]. A very effective technique for estimating elastic constants is the Mori–Tanaka approach. The extensive literature that employs this technique and the engineering programs that use it for design calculations provide confirmation. The Mori–Tanaka approach is used to glass-reinforced polyvinyl chloride (PVC) plastics, and the outcomes are contrasted with 3D numerical simulations for creep failure and creep deformation [107]. The Mori–Tanaka model's applicability in forecasting the impact of fiber length and fiber volume percentage on creep deformation and failure is confirmed by the comparison. Numerous applications and analyses of the Mori–Tanaka approach have been conducted [108–112]. The Mori–Tanaka homogenization method is used to study the linear elastic behavior of fiber-reinforced concrete (FRC) [113]. The overall stiffness estimates that were produced are extremely similar to the FEM-derived solutions. By comparing the model's results with those gained through experimentation in the literature, its validity is established. In [114], a novel homogenization model is put forth that employs incremental Mori–Tanaka schemes for high volume fractions and the viscoelastic constitutive law with an Eshelby micromechanical model. Direct numerical simulation and experimental DMA (dynamic mechanical analysis) results validate the model's simplicity and intuitiveness. Additional intriguing findings about the use of the Mori–Tanaka approach are provided in [115–122].

More developments in the field of fibrous composite materials studied using the Mori–Tanaka method and bounding methods (e.g., Hashin–Shtrikman bounds, Voigt–Reuss bounds) may cover a number of significant areas given the ongoing advances in multiscale modeling, materials design, and computational tools. The most promising directions are shown below:

- One of the directions is to more effectively predict effective qualities from microstructural data by integrating the Mori–Tanaka formalism with machine learning (ML) models.
- Other significant fields for future research or development of extended models for composites exposed to a couple of physical fields are multiscale and multi-physics modeling (e.g., piezoelectric fiber composites, magneto-active polymers).
- Nonlinear and time-dependent behavior are significant elements that need to be included in the models.
- Because of its simplicity, the bounded model is still useful in design. Composites with more irregular, graded, or hierarchical structures can benefit from improved bounding techniques for complicated microstructures.
- There is a wide range of applications for bio-inspired and smart composites, such as self-healing composites that use improved homogenization techniques or bio-inspired fiber designs.
- Digital twins and experimental validation represent an alternative approach that combines homogenization techniques with digital materials testing (such as X-ray CT + FEM) for real-time validation and feedback.

2.3. Homogenized Viscoelastic Coefficients

2.3.1. The Homogenization Method

The fundamental idea behind the homogenization theory is to create a homogeneous material with comparable macroscopic properties by modeling the behavior of the composite's complicated microstructure, which is typically a repeated structure. It is essential for modeling composites since they often have complex microstructures (such as fibers embedded in a matrix) and it is either too expensive or difficult to directly replicate every detail at large scales. A material is regarded as homogeneous and adheres to the theory of elasticity exactly like a homogeneous material even if it is fundamentally inhomogeneous but is composed at the microstructure level by identical, repeated, or specific symmetries.

Actually, the homogenization theory is a mathematical method for averaging the mechanical and physical properties of an inhomogeneous material. In many technological applications, homogenization theory is used to determine the properties of a body considered a solid composed of a homogeneous substance. The principles of this mathematical theory are outlined in [123–128]. Homogenization theory would help determine the total stiffness and strength of a fiber-reinforced composite material by taking into account the properties of both the fibers (which could be strong and stiff) and the matrix (which could be more flexible).

Homogenization enables an averaged material description that streamlines the analysis while preserving the fundamental behavior of the composite, as opposed to modeling each individual fiber and its interaction with the matrix. The ability of homogenization theory to evaluate differential equations with coefficients that change rapidly or frequently is one of its advantages. Engineering constants were obtained by averaging processes. A substance with a periodic structure can therefore be regarded as homogeneous. As a result, rather than using a differential equation with widely varying periodic coefficients, the modeling uses an equation with constant coefficients.

The traditional demonstration of Sanchez Palencia's homogenization technique is presented in [129–131]. The stress tensor σ^{δ} for a repeating unit cell (RVE) that makes up the composite, of size δ, must adhere to the traditional equations, taking into account the theory of elasticity hypothesis:

$$\begin{array}{l} \frac{\partial \sigma_{11}^{\delta}}{\partial x_1} + \frac{\partial \tau_{12}^{\delta}}{\partial x_2} + \frac{\partial \tau_{13}^{\delta}}{\partial x_3} = f_1(x); \\ \frac{\partial \tau_{21}^{\delta}}{\partial x_1} + \frac{\partial \sigma_{22}^{\delta}}{\partial x_2} + \frac{\partial \tau_{23}^{\delta}}{\partial x_3} = f_2(x); \\ \frac{\partial \tau_{31}^{\delta}}{\partial x_1} + \frac{\partial \tau_{32}^{\delta}}{\partial x_2} + \frac{\partial \sigma_{33}^{\delta}}{\partial x_3} = f_3(x), \end{array} \tag{22}$$

Because the tensor is symmetric, $\sigma_{ij}^{\delta} = \sigma_{ji}^{\delta}$, for $i, j = 1,\ 2,\ 3$.

$$u^{\delta}\Big|_{\partial_1 \Omega} = \widetilde{u}. \tag{23}$$

The boundary conditions on contour $\partial_2\Omega$, $(\partial_1\Omega \cup \partial_2\Omega = \partial\Omega)$ are as follows:

$$\begin{array}{l} \sigma_{11}^{\delta} n_1 + \tau_{12}^{\delta} n_2 + \tau_{13}^{\delta} n_3 = T_1(x); \\ \tau_{21}^{\delta} n_1 + \sigma_{22}^{\delta} n_2 + \tau_{23}^{\delta} n_3 = T_2(x); \\ \tau_{31}^{\delta} n_1 + \tau_{32}^{\delta} n_2 + \sigma_{33}^{\delta} n_3 = T_3(x). \end{array} \tag{24}$$

Hook's law it is written in the form:

$$\sigma^{\delta} = C\ \varepsilon^{\delta}. \tag{25}$$

These coefficients are derived by the use of averaging techniques. The process is described in [132,133]. These coefficients can be obtained in two ways:

- The homogenized coefficients are obtained after averaging the strain and stress field and calculating the averages using the local formulas;
- Finding a unique function that can assist us in figuring out the homogenized coefficients by applying the variational formulation.

In the first instance, it is necessary to obtain the field of stress and strain. These data must be acquired numerically because it is rarely possible to pinpoint the precise stress and strain field. The method that is most commonly used is the FEM.

2.3.2. Applications and Future Developments

The homogenization approach has been widely used to assess the mechanical behavior of unidirectional composites reinforced with continuous fibers. The field of stress and strain is identified in [132] using FEM. Additional findings that analyze a composite reinforced with carbon fibers using the traditional homogenization theory are provided in [133,134], along with experimental tests to confirm the findings. Ref. [130] introduces the use of homogenization theory for time-dependent nonlinear composites for creep analysis of polymer matrix composites. In [131], a homogenization approach based on Eshelby tensors is introduced, which makes it possible to compute the creep of fiber composites. Comparison with experimentally acquired data on the flow of the material under study validates the micromechanical model.

In numerous applications involving different types of resin and reinforcing materials, the homogenization theory has proven its capacity to yield precise and useful results.

Therefore, the effects of boundary conditions on carbon-fiber-reinforced polymer [135], the creep behavior of viscoelastic composites reinforced with long and short fibers [136], homogenization models for multi-scale problems for linearly viscoelastic 3D interlock woven composites [137], the anisotropic mechanical behavior of short fiber-reinforced composite [138] or long fiber-reinforced composite [139], or contemporary engineering applications like the use of Ti-based matrix composites reinforced by SiC fibers [140] were all investigated.

Numerous models have been produced by using mathematical methods of homogenization due to the various types of composite materials used in real-world applications [141–148].

It has been shown that the homogenization method and multiscale models are useful for investigating composite materials. The behavior of the material at the macroscale is influenced by loading conditions, environmental factors, and component behavior at the microscale [149–154].

Composite materials are used in many additional situations, with different geometric structures and materials, at different pressures, in different environments, and under long-term loads that call for creep investigations. Some of these are listed at [155–161].

The most important areas for future research development are as follows:

- A multi-scale or multi-physics modeling technique is a popular kind of study because of the computational capabilities that are currently available;
- Using Reduced Order Modeling (ROM) to lower high computational costs and further developing numerical calculation techniques like FE^2 (Finite Element Squared);
- Using ML-based constitutive models that can change over time and in response to damage, ML and AI are used to speed up the homogenization process;
- Directly include the high-resolution experimental data (SEM, micro-CT) into the homogenization process. Therefore, the creep strain field may be validated at various

scales using Digital Volume Correlation (DVC), and the RVEs can be directly constructed and introduced into numerical analysis using direct 3D scans;

- The evolution of micro-damage (cracking, fiber breaking) within homogenization methods is a crucial area of research.

All of these research method advancements have broad applications in CFRPs and GFRPs (in aerospace and automotive applications at high temperatures), C/Composites (where creep is crucial in thermal protection systems), Metal Matrix Composites (MMCs) (used for high-temperature structural applications), and Ceramic Matrix Composites (CMCs), where damage and creep are closely related.

Scientists and engineers can comprehend and predict the behavior of complex multiphase materials by using homogenization theory in composite materials, which reduces the system to an analogous homogeneous material. FEM proves to be a basic tool for studying the strain and stress field in materials in this case as well [162–171].

3. FEM Used to Compute the Elastic Constants of Composite Materials

3.1. FEM as a Useful Tool in the Determination of the Mechanical Properties of Composite

The main use of FEM is to determine the strain and stress field for structures (generally very simple) made of different types of composite materials. The main methods presented in the paper and used in practical applications by engineers and researchers require knowledge of these quantities. The method is well known by users and provides excellent results in most cases. The use of the method together with classical calculation methods has been presented in the previous sections. Next, we will present some ways of using FEM in specific practical cases and the help that the method can give for complex problems.

For the study of fractures in composite materials, FEM proves to be a useful tool. The crack introduces additional geometric elements [172]. Also the geometry of the interfaces is generally an element that must be taken into account. The paper proposes a multi-level approach and a technique for correcting the approximation in the mixing elements to solve this problem. Examples of two-dimensional and three-dimensional structures illustrate the method.

Delamination is an induced damage that occurs when composite materials are subjected to processes like turning, drilling, and milling. By reducing the operational variables and tool design, these damages can be minimized. The literature on composite machining is thoroughly reviewed in [173], with a primary focus on traditional techniques like turning, milling, cutting, and drilling as well as simulation techniques like the discrete element approach and finite element modeling. The findings are verified through experimentation.

Failures in fiber-reinforced composite materials (FRC) are complicated by the interaction of the constituents. In [174] a study of the damage behavior in a unidirectional epoxy resin reinforced with glass fibers is made. The study is carried out at both the micro and macro levels, using the finite element method. The isotropic elastic-brittle behavior and the Coulomb-Mohr criterion were applied to both the fiber and the epoxy resin. It was thus possible to predict the initiation of damage and the development of damage for the investigated FRC. Models based on the multiscale approach using finite elements are presented in [175,176]. Boundary integral equation methods interact closely with FEM. For details, see [177]. Pure FEM has essential disadvantages, particularly its inability to capture the correct singular behavior at crack tips and angular domains. Modern FEM packages incorporate asymptotic information derived from integral equation methods precisely to address these singularities.

FEM has also been used to predict the nonlinear behavior of composites [178]. An improved simple fixed-point iteration method is proposed to determine the stress field. This avoids the difficulties associated with convergence for large external loads. A practical

application exemplifies the proposed procedures. The same problem treated with FEM is presented in [179]. An augmented finite element method ("A-FEM") is used to study arbitrary discontinuities that cross the interior of elements [180]. This formulation is compatible with standard commercial FEM packages, which has the advantage of being able to model multiple discontinuities that occur on different surfaces. Various aspects involved in the use of composite materials are described in a rich literature [181–186]. The reference [187] enhances FEM with analytical formulas for the critical concentration of touching fibers and compares these with FEM computations across all inclusion concentrations.

3.2. FEM as a Method to Determine the Mechanical Properties

An example, presenting the mechanical behavior of polymer composite materials reinforced with randomly oriented short natural fibers with different proportions of the fiber volume fraction, will be analyzed through numerical simulations using the FEM [188,189].

The quasi-static case analyzed allows the loading history to be modeled using an incremental and iterative algorithm [190]. The discrete problem for each time increment may be nonlinear, and the linearization will be performed using the Newton–Raphson method. The model is analyzed for the case of a homogeneous and isotropic composite subjected to compression/tension forces for a flat plate supported on a rigid support under the assumption of plane strain conditions.

Variational formulations lead to incremental formulations by substituting (approximating) finite differences for the time derivatives of displacements. Step-by-step, quasi-static issues are handled by calculating minor stresses and small displacements, which are then added to the ones already calculated in the preceding step after modest incremental changes in the applied forces.

For the nondestructive experimental determination and verification through numerical simulation using direct and inverse methods, the following steps are performed:

- Experimental determination of the shear modulus of elasticity G by the resonance method, for specimens with a square cross-section, and by the identification method of the coefficients of the Euler–Bernoulli equation in the case of torsional vibrations;
- Experimental determination of the modulus of elasticity E by the first resonance method, for specimens with a rectangular cross-section, and by the identification method of the coefficients of the Euler–Bernoulli equation in the case of bending vibrations;
- Verification and comparison of the resonance frequency calculated using FEM (where the experimentally determined elastic constants were used) with the resonance frequency values determined experimentally.

3.2.1. Quasistatic Formulation of Problems in Composite Materials Reinforced with Randomly Oriented Short Fibers

We will analyze the case when given volumetric and tensile forces act on the bodies whose speed is sufficiently low that inertial effects can be neglected, i.e., the quasistatic case. Let us consider a viscoelastic composite body which, at time $t = 0$, has the domain $\subset \mathbb{R}^d$, where $d = 2$ or $d = 3$, with Lipschitz boundary $\partial\Omega = \overline{\Gamma}_u \cup \overline{\Gamma}_N$ decomposed into two mutually disjoint parts Γ_u, Γ_N, meas $(\Gamma_u) > 0$, (the measure of Γ_u is strictly positive, thus excluding rigid body motions). We denote $Q = \Omega \times [0, T]$, with $T > 0$, $S_u = \Gamma_u \times [0, T]$. The body is fixed on the boundary Γ_u where the displacement field is prescribed to be zero; that is, the body is clamped on this portion of the boundary. On the boundary Γ_N surface tractions of intensity $h(t)$ act. Volume forces of intensity $f(t)$ act in Ω (self-weight). The notations used are: $u(t) = (u_1, \ldots, u_d)$ the displacement vector, $\sigma = \{\sigma_{ij}\}$ the stress tensor, $\varepsilon(u(t)) = \{\varepsilon_{ij}(u(t))\}$ the strain tensor $i, j = 1, \ldots, d$,τ_N, τ_T şi u_N, u_T, the normal and

tangential components of the stress tensor and the displacement vector, respectively. We consider the Kelvin–Voigt constitutive relation in the viscoelastic case:

$$\sigma_{ij} \equiv \sigma_{ij}\left(u(t), \dot{u(t)}\right) = C^{(1)}_{ijkl}\varepsilon_{kl}(u(t)) + C^{(2)}_{ijkl}\varepsilon_{kl}\left(\dot{u}(t)\right); \tag{26}$$

where $C^{(1)}_{ijkl}$şi $C^{(2)}_{ijkl}$ cu $i, j, k, l = 1, \ldots, d$, are the components of the elastic and viscoelastic tensors, respectively, which satisfy the ellipticity condition.

The classical quasistatic equilibrium equations are the following:

$$-\text{div}\ \sigma(u(t)) = \text{f(t)},\ \text{in Q}; \tag{27}$$

$$\sigma\left(u(t),\ \dot{u(t)}\right) = C^{(1)}\varepsilon(u(t)) + C^{(2)}\varepsilon\left(\dot{u}(t)\right),\ \text{in Q}; \tag{28}$$

$$u(t) = 0 \text{ on } S_u; \tag{29}$$

$$\sigma{\cdot}n = h(t) \text{on } S_N; \tag{30}$$

$$u(x,\ 0) = u_0,\ \dot{u}\ (x, 0) = u_1 \text{on } S_u; \tag{31}$$

where n is the external normal unit on $\partial\Omega$, and $\dot{\boldsymbol{u}}(\boldsymbol{x}, t) = \frac{\partial \boldsymbol{u}(\boldsymbol{x},t)}{\partial t}$ is the deformation velocity.

Relation (27) is the equilibrium equation, (29) and (30) are the Dirichlet and Neumann boundary conditions, respectively, and (31) represents the initial conditions.

When studying the quasistatic problem, all data can depend on time. This aspect makes the studied process irreversible and dependent on the loading path. Thus, the final displacements and stresses depend on the way in which the volume forces $f(t)$ and the tractions $h(t)$ change in time and not only on their final values. The numerical algorithm proposed in this manuscript can describe this by making incremental loads, in small steps, followed by iterative solutions and testing the convergence of the method used.

The quasistatic problem with plane deformations for homogeneous and viscoelastic composite materials can be stated as follows:

Problem P1. *Determine the displacements and stresses that satisfy Equations (27)–(31) for any time t ∈ [0,1] and the initial condition u(x,0) = u_0 in Q.*

3.2.2. Variational Formulation of the Quasistatic Problem for Composite Materials

For the numerical solution of the quasistatic problem using the finite element method, a variational formulation is required. We begin by introducing the following function spaces:

$$V = \{v = (v_1, \ldots, v_d) \in [H^1(Q)]^d \mid v = 0 \text{ on } S_u\}; \tag{32}$$

$$a(u, \dot{u}, v) = \int_\Omega C^{(1)}_{ijkl}\varepsilon_{kl}(u)\varepsilon_{kl}(v)dx + \int_\Omega C^{(2)}_{ijkl}\varepsilon_{kl}\left(\dot{u}\right)\varepsilon_{kl}(v)\ dx; \tag{33}$$

$$F(u, v) = \int_\Omega f\ v\ dx + \int_{\Gamma_N} h\ v\ ds. \tag{34}$$

In order to obtain variational formulations, we will use Green's formulae, in which for $u, v \in V$, we get the following:

$$\int_\Omega C^{(1)}_{ijkl}\varepsilon_{kl}(u)\varepsilon_{kl}(v)dx + \int_\Omega C^{(2)}_{ijkl}\varepsilon_{kl}\left(\dot{u}\right)\varepsilon_{kl}(v)\ dx = a\left(u, \dot{u}, v\right). \tag{35}$$

For the numerical solution of the problems formulated above, it is necessary to consider approximations of these problems that are obtained through discretization with the finite element method in space and with finite differences in time. This procedure will lead to

incremental formulations, to which the same methods can be applied in principle as those applied to static problems.

3.2.3. Incremental Formulation Obtained by Temporal Discretization

The incremental formulations result from variational ones by replacing the time derivatives of the displacements with finite differences. Quasistatic problems are solved step by step, at each step, small deformations and small displacements are computed and added to the existing ones, obtained in the previous step, following small incremental changes in the applied forces.

Thus, within each increment, the dependence on the loading path is neglected, considering a sequence of such steps, also taking into account the way in which the applied forces vary over time.

To obtain incremental formulations of quasistatic problems, we introduce a partition $\left(t^0, t^1, \ldots, t^p\right)$ of the time interval $[0, T]$ and the following notations.

$$u(t^m) = u^m, \Delta u^m = u^{m+1} - u^m, \Delta t^m = t^{m+1} - t^m, F^m = F(t^m),$$
$$\Delta F^m = F^{m+1} - F^m, m = 0,\ 1,\ \ldots,\ p-1$$

The derivative, with respect to time t, is denoted by $\dot{\boldsymbol{u}}(\boldsymbol{x}, t) = \frac{\partial \boldsymbol{u}(\boldsymbol{x},t)}{\partial t}$ is approximated using the finite difference formula:

$$\dot{u}(t^m) \cong \frac{u\left(t^{m+1}\right) - u(t^m)}{t^{m+1} - t^m} = \frac{\Delta u^m}{\Delta t^m},\ m = 0,\ 1,\ \ldots,\ p-1$$

Using the above notations, the time-discretized form of Problem P'1 will become

$$a\left(u^m + \Delta u^m, \frac{\Delta u^m}{\Delta t^m}, v - \frac{\Delta u^m}{\Delta t^m}\right) \geq \left(F^m + \Delta F^m\right)\left(v - \frac{\Delta u^m}{\Delta t^m}\right) \tag{36}$$

Problem P'1. *Find out* $\Delta\, \boldsymbol{u}^m \in V$ *so that*

$$a(\Delta u^m, \Delta u^m, w - \Delta u^m)\Delta F^m(w - \Delta u^m) - G(u^m, w - \Delta u^m), \forall w \in K^m \tag{37}$$

where we denoted

$$G\ (u^m,\ w - \Delta\ u^m) = a\ (u^m,\ \Delta\ u^m,\ w - \Delta\ u^m) -\ F^m\ (w - \Delta\ u^m)$$

The incremental problem becomes the following:

It is required to find out the sequence $\boldsymbol{u}^1,\ \ldots,\ \boldsymbol{u}^p$ *with* $\boldsymbol{u}^{m+1} = \boldsymbol{u}^m + \Delta \boldsymbol{u}^m \in V,\ \left(\boldsymbol{u}^0 = \boldsymbol{u}_0\right)$, *where* $\Delta \boldsymbol{u}^m \in V$ *is the solution of the inequality.*

$$a\ (\Delta\ u^m,\ \Delta\ u^m,\ w - \Delta\ u^m) \geq\ F^m\ (w - \Delta\ u^m) - G\ (u^m,\ w - \Delta\ u^m)\ \forall\ w \in V. \tag{38}$$

In order to correctly model these characteristics, the incremental and iterative Newton–Raphson method was used.

3.2.4. Finite Element Approximation and Description of Iterative Incremental Algorithms

Using the standard procedure for the finite element method, the approximation of the variational Equation (38) can be performed in the finite-dimensional space $V_h \subset V$. For a given $h > 0$, which defines the fineness of the partition, the displacement approximations for time $t \in [0, T]$ are elements, $\boldsymbol{u}^h(x, t) \in V_h$. Within each finite element $\Omega_h^e (e = 1,\ \ldots,\ N_h)$ of

Ω, the displacement field inside the finite element is interpolated between its nodal values as follows:

$$u_d(x,t) = \sum_{i=1}^{N_e} u_d^i(t) N_d(x), \tag{39}$$

where $d = 2$ or 3, N_e- is the number of nodes of the finite element Ω_h^e, and N_d is the interpolation function. For each incremental step, the Problem P"2 is obtained, and if we consider an internal approximation $(V_h,\ K_h)$ of finite element type, with a discretization parameter $h > 0$ [164,191], we have:

Problem P"2h. *Find* $\boldsymbol{u}_h^m$ *such that*

$$a(u_h^m,\ u_h^m,\ w_h - u_h^m) \geq F_h^m(w_h - u_h^m) - G\ (u_h^m,\ w_h - u_h^m). \tag{40}$$

Considering that for each time increment Δt*, is obtained a static problem, the existence of the finite element approximate solution reduces to proving the existence of a solution* $\boldsymbol{u}_h^m$ *of inequality (40) which is a fixed point of the function* $f_h : K_h \to K_h$ *associating to every* $\boldsymbol{z}_h^m \in K_h$ *the element* $f_h \boldsymbol{z}_h^m \in K_h$*, defined by*

$$a(f_h z_h^m,\ f_h z_h^m,\ w_h - f_h z_h^m) \geq F_h^m(w_h - f_h z_h^m) - G\ (f_h z_h^m,\ w_h - f_h\ z_h^m),\ \forall\ w_h \in\ V_h \tag{41}$$

so that the sequence $\left\{\boldsymbol{w}_{hn}^m\right\}$ *converges to* $\boldsymbol{w}_h^m$*, where* $\boldsymbol{w}_{hn}^m = f_h\ \boldsymbol{w}_{h(n-1)}^m,\ n \geq 1,$ *because the function* f_h *is a contraction.*

The matrix formulation of the equilibrium equation, approximated by the finite element method for Problem P"2h, has the form:

Problem P"2hm. *Find the solution* $U : [0,T] \to \mathbb{R}^{dxN_t^\Omega}$ *such that*

$$K\ U(t) = F(t), t\ \in [0,T]; \tag{42}$$

where (42) is an algebraic system of equations obtained by approximation of the spatial variables using the finite element method and the temporal variables with finite differences.

Matrix K is the stiffness matrix, and $F(t)$ *is the load vector obtained from (37) and (38) through finite element approximation and assembly.*

3.3. Use of FEM in the Vibration Analysis in Order to Determine the Engineering Constants

We will exemplify with a simple example, with a FEM model to calculate the natural frequencies of a beam embedded at both ends. The material from which the beam is made is a polymer composite reinforced with carbon fibers. Within the standard assumptions of the classical theory of straight bars, with the values determined based on the formulas provided by the literature and knowing the values of the eigenpulsations determined with the FEM model, the Young's modulus or other constants can be determined. The study of the identification of the material properties using an inverse method is presented in [192].

The main advantage offered by this method is that it provides quick and good estimates. Obviously, the costs involved are also reduced. If it is compared with the experimental methods, the method is much cheaper and more convenient. Also, the time required to obtain these values is reduced. The analysis focuses on the study of torsional vibrations. The method can be applied to a wide class of materials in order to determine the properties of the homogenized material. The resonance method enables the determination of material constant variation (for the modulus of elasticity E and the shear modulus G), using the updated values to model realistic mechanical behavior through FEM-based inverse approaches. The connection between the non-destructive testing (NDT) method and FEM

analysis can provide a more accurate modeling of this behavior, as damage occurs during the loading of composite materials, leading to a reduction in the elastic moduli of the constituent materials. The generalized inverse method can be applied to many composite materials, including those with synthetic fibers or hybrid fiber–matrix systems.

The FEM is first used to determine the natural frequencies for a composite material, using all the information regarding the matrix material and the fiber material in the modeling. At the same time, the classical methods are considered for determining the natural frequencies for a straight bar, made of the same material, which represents the homogenized material having the properties determined by the properties of the phases used. By comparing these values and comparing with those obtained using FEM, the values for the elastic constants for the homogenized material can be obtained. The classic assumptions from the straight bar theory are considered valid [74]. Knowing the relations that provide the analytical expression of the eigenfrequencies of a homogeneous beam depending on the dimensions of the beam and the Young's modulus and having the eigenfrequencies calculated with the FEM, it is possible to obtain the Young's modulus from these relations through simple calculations. Figure 3 shows the two types of beams analyzed.

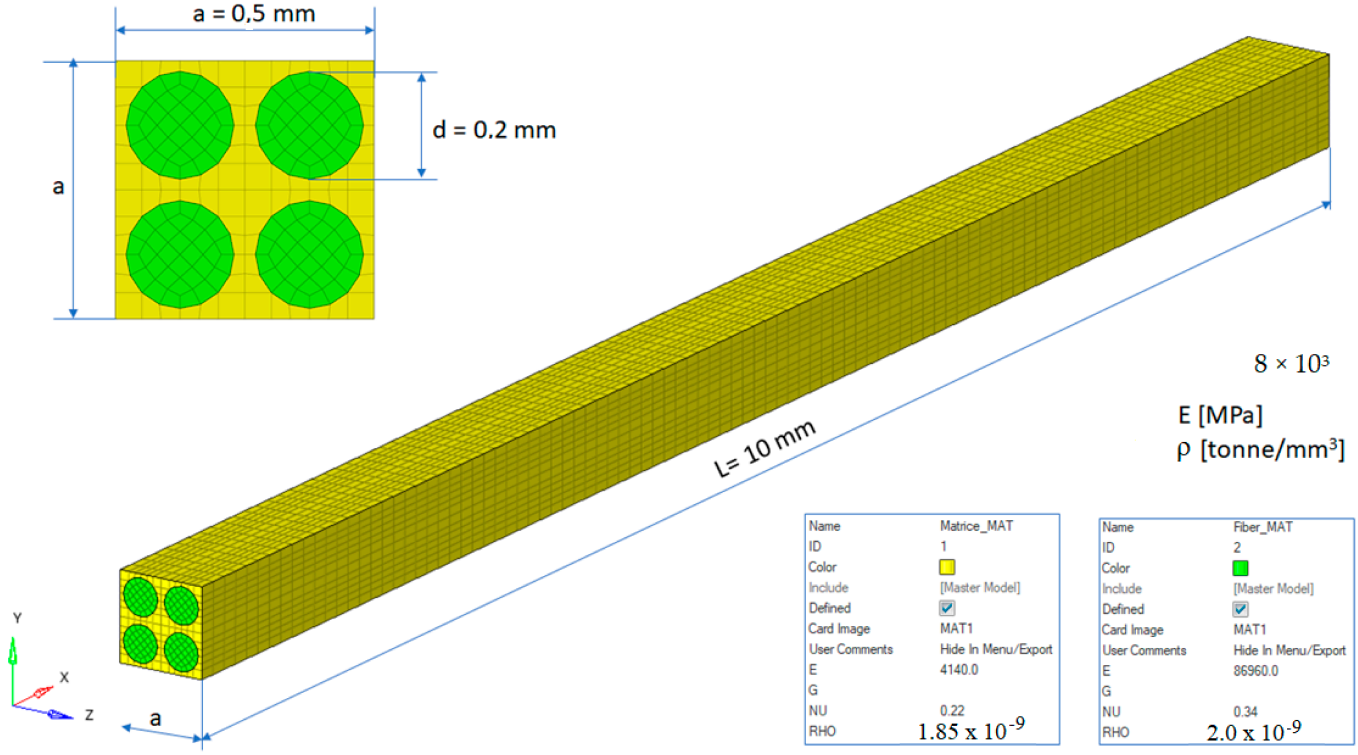

Figure 3. Beam clamped at both ends.

Considering the torsional vibration of a straight beam, the eigenpulsation is obtained using the classic formula:

$$p_n = \frac{n\pi}{l}\sqrt{\frac{G}{\rho}}\ ;\ n = 1,\ 2,\ 3, \ldots\ldots$$

So the shear modulus of the homogenized material clamped at both ends can be determined:

$$G = \frac{p_n^2\, l^2 \rho}{n^2 \pi^2}\ ;\ n = 1,\ 2,\ 3, \ldots\ldots \tag{43}$$

From Equation (43), it results in the following:

$$p_1 = \frac{p_2}{2} = \frac{p_3}{3} = \ldots\ldots = \frac{p_n}{n} = ct\ ;\ n = 1,\ 2,\ 3,\ldots\ldots \tag{44}$$

Using FEM, it is possible to obtain a number of eigenpulsations which offer us more values for G. The average can be calculated in order to obtain a better estimation for G (Table 2).

The engineering constants for a composite material reinforced with fibers can be quickly estimated using the method suggested in this paper. Designers may find the method helpful in obtaining the data required for the design process. This approach makes use of FEM, a calculation technique that designers have learned and that yields accurate results. The shear modulus is then calculated using the eigenpulsations for the examined specimen. The characteristics of the phases that comprise the composite must be understood. One argument in favor of this method's application during the design process is its ease of use and quickness. FEM errors, which are essentially an approximation method, and the approximations and assumptions made in the traditional calculation of the straight beam, have the biggest impact on the estimate. In the example examined in the paper, the outcomes are comparable to those produced by alternative techniques and then confirmed through experimentation [193,194]. It goes without saying that the model can be enhanced if Young's modulus needs to be calculated for unique circumstances or if the impact of temperature, humidity, or other variables needs to be considered.

Table 2. Eigenpulsation of the torsional vibration $p_n = \frac{n\pi}{l}\sqrt{\frac{G}{\rho}}\ ;\ n = 1,\ 2,\ 3,\ldots\ldots$

Mode No.	Eigenpulsations [Hz]	Representation	$G=\frac{p_n^2 l^2 \rho}{n^2\pi^2}$ [GPa}
3	82,288.62	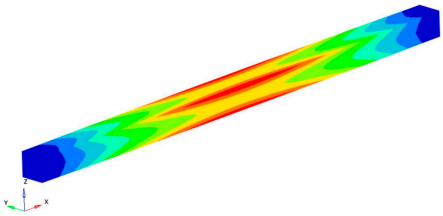	13,172.86
5	164,757.2	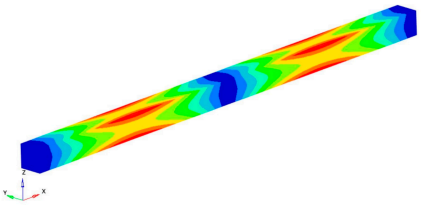	13,201.68
8	247,584.1	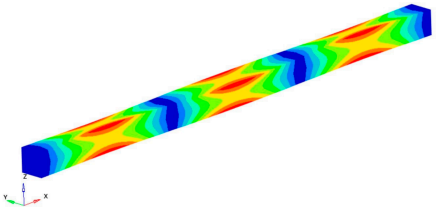	13,249.62

Table 2. *Cont.*

Mode No.	Eigenpulsations [Hz]	Representation	$G=\frac{p_n^2 l^2 \rho}{n^2 \pi^2}$ [GPa}
11	330,944.5	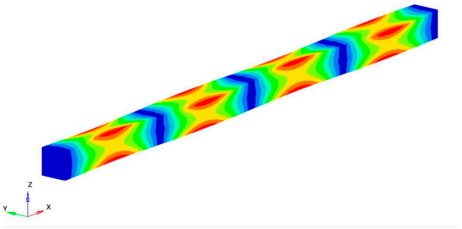	13,316.52
13	415,008.4	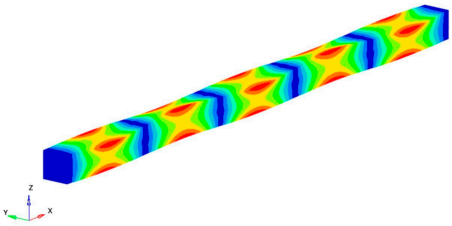	13,402.14
15	499,938.3	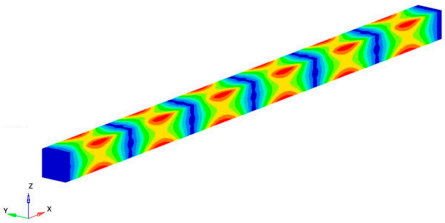	13,506.13
18	585,886.5	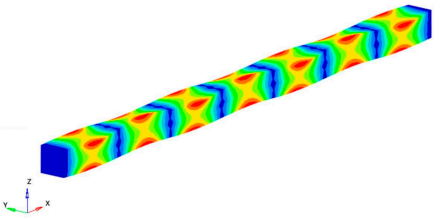	13,627.98
20	672,992.2	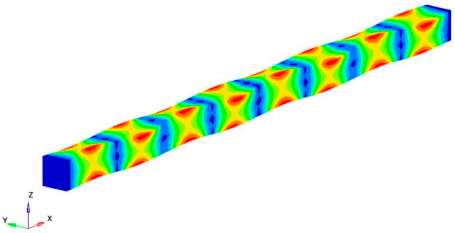	13,767.04
	Average shear modulus [GPa]		13,405.50

4. Discussion and Conclusions

Even though the mechanical behavior of fiber-reinforced composites is commonly studied using the FEM, there is still a great expectation of unrealized research potential in this field. These are some promising directions for future study on the mechanical properties of fiber composites using FEM.

FEM is the primary numerical tool for the investigation of fiber composite materials because of their structural complexity and anisotropic mechanical behavior. The field's literature highlights the method's development and application directions. We discuss the main steps for method application development.

The link between the global structural response and the microstructural behavior (fibers, matrix, interface) is made possible by multi-scale modeling. Effective attributes are determined using representative volume elements (RVEs) at the micro level and then incorporated into macro-scale assessments. The impact of fiber distribution, orientation, and microscopic flaws on the overall mechanical properties can thus be examined. Therefore, it is possible to establish hierarchical or concurrent multiscale FEM models by connecting microscale material behavior with macroscale performance.

A computational homogenization method that combines two layers of finite element analysis is called Finite Element Squared (FE^2). The overall structural behavior of the composite material represents the first level at the macroscopic scale. At the microscopic level, the second level depicts the intricate behavior of the material's microstructure, including interactions between fibers and matrices. Because it can capture both macroscopic and microscopic responses, FE^2 offers a comprehensive, physics-based method for modeling creep behavior. Materials whose behavior is dependent on intricate microstructures can be numerically homogenized using this method. It accomplishes this by concurrently solving finite element models at the macro and micro scales. The following process is used to do this. The macro-model discretized using conventional finite elements is taken into consideration first. Next, an RVE is assigned to each Gauss point taken into account throughout the discretization process. The internal structure of the material (fibers, voids, etc.) is depicted in this microscale model. The RVE is subject to the boundary conditions. Calculations are made for the microscale stress response, which may include creep, damage, plasticity, etc. The average stress from the RVE is now fed back into the macro-model to continue solving the macro-problem. This macro/micro two-way communication is included in every time step and is especially important for time-dependent problems like creep. When analyzing creep, a time-dependent deformation under constant stress, FE^2 allows the simulation of both immediate and long-term material reactions by simultaneously accounting for both scales. The FE^2 (Finite Element Squared) method is a multiscalar approach that can be used to study complex materials. The behavior at the microscopic scale directly influences the response at the macroscopic scale. The microscopic model contains real details about the fibers, matrix, and geometry of the structure. This model is also discretized with finite elements. The deformations determined at the macro level are transmitted to the micro model, which will solve the local problem and return the average stress values. These results are used back in the macro-model. The iteration process continues as long as necessary.

However, the method has some drawbacks: it is very computationally expensive because you are solving an RVE problem for each Gauss point and time step; it is not feasible for large structures or long-term creep simulations without parallel computing or reduced-order models; and it is difficult to implement FE^2 and is typically done in advanced research codes (such as in-house solvers or frameworks like MultiscaleFE, MFront, or FEAP).

The behavior at the fiber-matrix interface may also become significant for contemporary applications. This is accomplished by applying laws for the interface's progressive degradation over time or with use, as well as by using models to analyze cohesiveness and delamination. This makes it possible to use FEM to simulate damage initiation and propagation in parallel.

The nonlinear behavior of the matrix remains a problem that has not been definitively solved and always requires new efforts for study. Also, progressive and cumulative damage such as fiber breakage can now be modeled appropriately using commercial FEM programs. The development of nonlinear and viscoelastic/viscoplastic constitutive models is necessary to integrate advanced time-dependent constitutive models (e.g., Schapery, Findley, or Anand-type models) into FEM codes for better prediction accuracy under various loading histories.

The development of benchmarked datasets and the promotion of FEM-experiment hybrid research, particularly with digital image correlation (DIC) and in situ microscopy techniques, is driven by the validation of the results or lengthy duration models.

The main problem faced by composite material manufacturers is the significant dispersion of composite material properties. This disturbing reality requires the coupling of FEM-type calculation methods with probabilistic methods (Monte Carlo, stochastic FEM, structural reliability). This type of analysis allows for increasing the safety in the design of such structures. Complex fiber orientations and voids can be introduced by additive manufacturing (3D printing). It may be useful to use FEM to investigate the effects of non-traditional fiber topologies on creep and use simulation to optimize them for long-term reliability.

Obviously, the development of the use of artificial intelligence also impacts this field. An accelerated integration of FEM with artificial intelligence and machine learning techniques is observed. This mode of analysis allows for accelerating mechanical predictions, optimizing fiber architecture and reducing computational costs.

The application of FEM to industrial process simulation is a new avenue. Such a study can be used to assess resin flow, calculate residual stresses, and establish a relationship between the final mechanical properties and the production process.

Natural fiber composites have unique qualities and are growing in popularity. When simulating creep in biocomposites, FEM systems must be adjusted to take into consideration environmental factors such as moisture and biodegradation.

Creep testing processes can be optimized while saving money and time with the use of digital twins and accelerated testing. Virtual models of composite parts can continuously simulate creep behavior by using real-time data input. In the automotive and aerospace sectors, digital twins can be used to monitor and predict damage from creep in real time. "Digital twins", as virtual models that faithfully replicate the behavior of a physical system in real or near real time, can be of real use in the study of composites. They are useful for design, analysis and optimization, especially in basic fields such as aerospace, automotive or construction engineering. It is possible to replicate a composite's layered structure, microscopic flaws, or thickness fluctuations. Traction, compression, fatigue, and impact are examples of real stressors that are emulated. Without conducting thorough physical testing, the data enable the prediction of the material's behavior or failure. Therefore, it is possible to determine the best configurations for strength and minimum weight by taking into account multiple circumstances. When sensors are incorporated into mechanical structures, the data gathered updates the digital twin in real time, enabling quick model recalibration, predictive maintenance, and degradation detection. New applications such as the study of random composites remain a new field of research with many interesting problems [187,195–197]. Paper [196] corrects Hill's classical concept [1,2] of the Representative Volume Element. It rigorously demonstrates that the RVE must be a periodicity parallelogram; other shapes may lead to incorrect values of the effective material constants. This important clarification should be taken into account in our analysis.

The extension of FEM, by breaking the classical calculation framework, towards multi-physics analyses (thermo-mechanical, electro-mechanical, fluid-structural) allows for promising perspectives for the development of functional composite materials and intelligent structures, capable of real-time monitoring and adaptation.

Author Contributions: Conceptualization, M.L.S., S.V. and P.N.; Methodology, M.L.S.; Software, M.L.S., S.V. and A.M.M.; Validation, M.L.S., S.V., P.N. and T.S.; Formal Analysis, M.L.S., P.N. and A.M.M.; Investigation, M.L.S., A.M.M. and V.M.M.; Resources, M.L.S., A.M.M., T.S. and V.M.M.; Data Curation, M.L.S., P.N., A.M.M. and T.S.; Writing—Original Draft Preparation, M.L.S., S.V. and P.N.; Writing—Review and Editing, M.L.S. and P.N.; Visualization, S.V., P.N. and T.S.; Supervision, S.V.,

P.N. and A.M.M.; Project Administration, M.L.S. and S.V.; Funding Acquisition, M.L.S. and S.V. All authors have read and agreed to the published version of the manuscript.

Funding: The APC was funded by Transilvania University of Brasov, HBS 2671/2020.

Institutional Review Board Statement: Not applicable.

Informed Consent Statement: Not applicable.

Data Availability Statement: The original contributions presented in the study are included in the article; further inquiries can be directed to the corresponding authors.

Acknowledgments: The authors wish to express their gratitude to the Ministry of Education and Research, CCCDI—UEFISCDI, for supporting the project PN-IV-P6-6.1-CoEx-2024-0162, within PNCDI IV.

Conflicts of Interest: The authors declare no conflicts of interest.

Appendix A. Basic Considerations and Notations

Appendix A.1. Behavior of Composites in the Elastic Domain

General Considerations

The section aims to provide a brief presentation of the principles underlying the calculation of composite materials and the main (and most frequently used) notations. There is a multitude of presentations and notations in this field, which is why we have tried to present the theoretical part of the field very briefly, with the notations most used by researchers for applications in the engineering field.

The possibility of combining materials with different properties to obtain a material with certain desired characteristics represents the advantage of a composite material.

The fibers used in polymer matrix composites can be glass, metal, carbon, or organic fibers. For each of these families, a wide range of mechanical properties can be obtained, depending on the way the fibers are obtained. Glass and metal fibers are isotropic, so their mechanical properties will be defined by two parameters.

Carbon and organic fibers, due to molecular alignment, are transversely isotropic and five parameters are required to define the mechanical properties.

Polymer matrices can be manufactured in two ways. The first way consists of a "casting" of the material which, after cooling, solidifies (thermoplastic materials). The other way consists of the irreversible solidification of the material following chemical reactions that lock the molecular structures in a three-dimensional network. These materials cannot be "cast". The upper limit at which a polymer can be used is determined by the "glass transition temperature" Tg. At temperatures above this limit, the stiffness of some polymers decreases by several orders of magnitude. In the present study, it will be considered that the polymers will be isotropic materials, so only two parameters are needed to define the elastic properties. In general, there is a large difference between the quantities that define the elastic properties of the fibers and the matrix.

The microstructure, i.e., the way the reinforcement material is arranged in the matrix, will determine the properties of the resulting material. In a composite with fibers, these can be long and aligned, packed according to a certain geometry, can have a circular or elliptical cross-section or there can be composites with short fibers. For short fibers, the spatial arrangement is determined by the way in which the composite material will be manufactured. Variations in the orientation of the fibers and in their length, determined by the manufacturing process, can lead to significant variations in the mechanical properties of the resulting composite material. This means that we can obtain a great diversity of properties of the composite material, using only two constituents but varying the dimensions and orientation of one of them.

The central problem in developing a mechanical model of a composite consists of determining a field of deformations (stresses) consistent with the field imposed on the body at the macroscopic level. The field of stresses and deformations of a homogeneous body, at the macroscopic level, can be obtained if the contour conditions imposed on the body and the loading that requires it are taken into account. The loads and deformations at the dividing contour of the elements that make up the composite are generally difficult to obtain. The internal field of stresses and strains at the microscopic level is locally influenced by the relative difference between the properties of the constituents, their size, shape and relative orientation as well as the geometry of the arrangement of the cells that are repeated to form the composite.

Although the materials that make up a composite material can be isotropic, due to their arrangement, the resulting material can be, on average, anisotropic. The materials that are used in practice can be homogeneous or inhomogeneous materials. A composite material is, obviously, inhomogeneous. However, within the models that are developed to determine the elastic properties of a composite, it is considered that, on average, we are dealing with a homogeneous material, generally anisotropic. The inhomogeneous material results from the statistical arrangement of the reinforcing materials within the bonding matrix.

An anisotropic body has different properties along different directions. The directions for which the elastic properties are the same are said to be elastically equivalent. Depending on its structure a body can be isotropic or anisotropic and homogeneous or inhomogeneous. In the different types of materials, two types of anisotropy can be distinguished: linear and nonlinear.

Appendix A.2. Anisotropic Elasticity

The relationship between stresses and strains is established by the constitutive equations, determined experimentally. If we place our considerations within the framework of linear elasticity, the relationship between stresses and strains will be linear and we can write the generalized Hooke's law in the form:

$$\{\sigma\} = \begin{Bmatrix} \sigma_{11} \\ \sigma_{22} \\ \sigma_{33} \\ \sigma_{12} \\ \sigma_{23} \\ \sigma_{31} \end{Bmatrix} = \begin{bmatrix} C_{11} & C_{12} & C_{13} & C_{14} & C_{15} & C_{16} \\ C_{21} & C_{22} & C_{23} & C_{24} & C_{25} & C_{26} \\ C_{31} & C_{32} & C_{33} & C_{34} & C_{35} & C_{36} \\ C_{41} & C_{42} & C_{43} & C_{44} & C_{45} & C_{46} \\ C_{51} & C_{52} & C_{53} & C_{54} & C_{55} & C_{56} \\ C_{61} & C_{62} & C_{63} & C_{64} & C_{65} & C_{66} \end{bmatrix} \begin{Bmatrix} \varepsilon_{11} \\ \varepsilon_{22} \\ \varepsilon_{33} \\ 2\varepsilon_{12} \\ 2\varepsilon_{23} \\ 2\varepsilon_{31} \end{Bmatrix} = [C]\{\varepsilon\} \tag{A1}$$

If the material is homogeneous, the coefficients C_{ij} are constant for the entire volume. If we are dealing with an inhomogeneous body, then the coefficients will depend on the position of the point considered. In the case of a homogeneous body, the coefficients C_{ij} will be called elastic constants or elastic moduli. In the case of an inhomogeneous body, these coefficients will be called elastic characteristics. In the case of the work, homogeneous materials will be considered.

The relationship between deformations and stresses can also be obtained by inversion of matrix [*C*]:

$$\{\varepsilon\} = [C]^{-1}\{\sigma\} = [S]\{\sigma\}. \tag{A2}$$

The matrix $[S]$ is called the compliance matrix and the coefficients S_{ij}, which are also elastic constants, are called the specific strain coefficients or compliance constants. To determine the stress–strain relationship, it is generally necessary to know 36 elastic parameters. The equations written are valid for linear elastic, homogeneous and anisotropic

materials. For this type of material, the matrices $[C]$ and $[S]$ are symmetric. From this consideration it follows that such a matrix is defined by only 21 elastic constants that will have to be determined experimentally.

Some authors use, instead of elastic constants, the so-called engineering constants such as Young's modulus, shear modulus of elasticity, and Poisson's ratio.

If there is a certain type of symmetry for an anisotropic body, then the generalized Hooke's law simplifies its form since a series of terms become zero, while there are linear connections between others. In the following, the main types of elastic symmetry encountered in practice will be presented.

(a) Plane of elastic symmetry

Let us assume that through each point of the body passes a plane that has the following properties: any two directions that are symmetrical about this plane are equivalent in terms of elastic properties. A direction perpendicular to the plane of elastic symmetry will be called the principal direction of elasticity.

If the x-axis is chosen to be normal to the plane of elastic symmetry and the other two axes in the plane, then eight elastic constants will have to be zero. If we write the relationship between elastic deformations and stresses in the form

$$\{\varepsilon\} = [C]^{-1}\{\sigma\} = [S]\{\sigma\}$$

we will have to have:

$$S_{14} = S_{24} = S_{34} = S_{46} = S_{15} = S_{25} = S_{35} = S_{56} = 0, \tag{A3}$$

and the number of elastic constants will be restricted to 13.

(b) Orthotropic body

If three perpendicular planes of elastic symmetry pass through each point of the body and these planes maintain their orientation at any point of the body, we say that we are dealing with an anisotropic orthogonal body or, in short, orthotropic. If we consider the other main elastic directions, we will have to have, in addition to the previous case, the following conditions:

$$S_{14} = S_{24} = S_{34} = S_{56}. \tag{A4}$$

and by virtue of the symmetry of the coefficient matrix, they will depend only on nine parameters. If the engineering constants E_{ii}, G_{ij}, ν_{ij} are introduced, the relationships between deformations and stresses, for a body with orthotropic elasticity, are as follows:

$$\{\varepsilon\} = \begin{Bmatrix} \varepsilon_{11} \\ \varepsilon_{22} \\ \varepsilon_{33} \\ 2\varepsilon_{23} \\ 2\varepsilon_{31} \\ 2\varepsilon_{12} \end{Bmatrix} = \begin{bmatrix} \frac{1}{E_{11}} & -\frac{\nu_{21}}{E_{22}} & -\frac{\nu_{31}}{E_{33}} & 0 & 0 & 0 \\ -\frac{\nu_{12}}{E_{11}} & \frac{1}{E_{22}} & -\frac{\nu_{32}}{E_{33}} & 0 & 0 & 0 \\ -\frac{\nu_{13}}{E_{11}} & -\frac{\nu_{23}}{E_{22}} & \frac{1}{E_{33}} & 0 & 0 & 0 \\ 0 & 0 & 0 & \frac{2}{G_{23}} & 0 & 0 \\ 0 & 0 & 0 & 0 & \frac{2}{G_{31}} & 0 \\ 0 & 0 & 0 & 0 & 0 & \frac{2}{G_{12}} \end{bmatrix} \begin{Bmatrix} \sigma_{11} \\ \sigma_{22} \\ \sigma_{33} \\ \sigma_{23} \\ \sigma_{31} \\ \sigma_{12} \end{Bmatrix} \tag{A5}$$

Between the coefficients E_{ij} there are the following relationships, dictated by the symmetry of the coefficients:

$$\frac{\nu_{12}}{E_{11}} = \frac{\nu_{21}}{E_{22}}\ ;\ \frac{\nu_{23}}{E_{22}} = \frac{\nu_{32}}{E_{33}}\ ;\ \frac{\nu_{31}}{E_{33}} = \frac{\nu_{13}}{E_{11}}\ ; \tag{A6}$$

which reduces the number of independent engineering constants from 12 to nine.

(c) Isotropy plane (axis of rotation symmetry)—transversely isotropic body

Let us consider a body that has the following properties: through each point pass parallel elastic symmetry planes, in which all directions are elastically equivalent (isotropic plane). In other words, at each point there is a principal direction of elasticity with a fixed direction at any point of the body and an infinity of principal directions of elasticity in the plane normal to this direction. Such a body therefore possesses cylindrical symmetry with respect to elastic properties. It is called transversely isotropic.

If we introduce the engineering constants E_L, E_T the transverse Young's moduli along the axis of cylindrical symmetry and along a direction in the isotropy plane, ν_T Poisson's ratio characterizing the transverse contraction in the isotropy plane when the stress is applied in this plane, ν_L Poisson's ratio characterizing the transverse contraction in the isotropy plane when the stress is applied in the normal direction to the isotropy plane, G_T is the shear modulus of elasticity for the isotropy plane and G_L the shear modulus of elasticity for a plane perpendicular to the isotropy plane. In this case we can write the following:

$$\{\varepsilon\} = \begin{Bmatrix} \varepsilon_{11} \\ \varepsilon_{22} \\ \varepsilon_{33} \\ 2\varepsilon_{23} \\ 2\varepsilon_{31} \\ 2\varepsilon_{12} \end{Bmatrix} = \begin{bmatrix} \frac{1}{E_L} & -\frac{\nu_T}{E_T} & -\frac{\nu_T}{E_T} & 0 & 0 & 0 \\ -\frac{\nu_L}{E_L} & \frac{1}{E_T} & -\frac{\nu_T}{E_T} & 0 & 0 & 0 \\ -\frac{\nu_L}{E_L} & -\frac{\nu_T}{E_T} & \frac{1}{E_T} & 0 & 0 & 0 \\ 0 & 0 & 0 & \frac{2}{G_T} & 0 & 0 \\ 0 & 0 & 0 & 0 & \frac{2}{G_L} & 0 \\ 0 & 0 & 0 & 0 & 0 & \frac{2}{G_L} \end{bmatrix} \begin{Bmatrix} \sigma_{11} \\ \sigma_{22} \\ \sigma_{33} \\ \sigma_{23} \\ \sigma_{31} \\ \sigma_{12} \end{Bmatrix}, \tag{A7}$$

with

$$C_{66} = \frac{C_{22} - C_{23}}{2}. \tag{A8}$$

(d) Isotropic body

If all directions are elastically equivalent and principal, then the result for Hooke's law will have the well-known form:

$$\begin{gathered} \varepsilon_{11} = \frac{1}{E}[\sigma_{11} - \nu(\sigma_{22} + \sigma_{33})]\,; \varepsilon_{22} = \frac{1}{E}[\sigma_{22} - \nu(\sigma_{33} + \sigma_{11})]\,; \\ \varepsilon_{33} = \frac{1}{E}[\sigma_{33} - \nu(\sigma_{11} + \sigma_{22})]\,; \end{gathered} \tag{A9}$$

$$\begin{gathered} \gamma_{12} = 2\varepsilon_{12} = \frac{2(1+\nu)}{E}\sigma_{12}\,; \\ \gamma_{23} = 2\varepsilon_{23} = \frac{2(1+\nu)}{E}\sigma_{23}\,;\ \gamma_{31} = 2\varepsilon_{31} = \frac{2(1+\nu)}{E}\sigma_{31}\,. \end{gathered} \tag{A10}$$

where E is the Young's modulus, ν is Poisson's ratio and G represents the shear modulus of elasticity, which, for isotropic materials, is given by the relationship:

$$G = \frac{E}{2(1+\nu)}. \tag{A11}$$

Lamé's constant λ has the expression:

$$\lambda = \frac{2G\nu}{1-2\nu} = \frac{E\nu}{(1+\nu)(1-2\nu)}\,. \tag{A12}$$

The strain is as follows:

$$\varepsilon_v = \varepsilon_{11} + \varepsilon_{22} + \varepsilon_{33}, \tag{A13}$$

and the relationships between stresses and strain can be written as follows:

$$\sigma_{11} = \lambda\varepsilon_v + 2G\varepsilon_{11}\,;\ \sigma_{22} = \lambda\varepsilon_v + 2G\varepsilon_{22}\,;\ \sigma_{33} = \lambda\varepsilon_v + 2G\varepsilon_{33}\,;. \tag{A14}$$

$$\sigma_{12} = 2G\varepsilon_{12}\ ;\ \sigma_{23} = 2G\varepsilon_{23}\ ;\ \sigma_{31} = 2G\varepsilon_{31}\ ;. \tag{A15}$$

Appendix A.3. Relationships Between Elastic Constants

Common engineering elastic constants are Young's modulus (longitudinal modulus of elasticity), Poisson's ratio, and shear modulus of elasticity. In the following, we will present the relationships that exist between these material constants and the coefficients that appear in the generalized Hooke's law for isotropic and transversely isotropic materials.

Appendix A.3.1. Isotropic Materials

The constitutive law for an isotropic material is as follows:

$$\sigma_{ij} = \lambda\ \varepsilon_{kk}\delta_{ij} + 2G\varepsilon_{ij}, \tag{A16}$$

or, explicitly

$$\begin{aligned} \sigma_{11} &= \lambda(\varepsilon_{11} + \varepsilon_{22} + \varepsilon_{33}) + 2G\varepsilon_{11} \\ \sigma_{22} &= \lambda(\varepsilon_{11} + \varepsilon_{22} + \varepsilon_{33}) + 2G\varepsilon_{22} \\ \sigma_{33} &= \lambda(\varepsilon_{11} + \varepsilon_{22} + \varepsilon_{33}) + 2G\varepsilon_{33} \end{aligned} \tag{A17}$$

$$\sigma_{12} = 2G\varepsilon_{12}; \sigma_{23} = 2G\varepsilon_{23}; \sigma_{31} = 2G\varepsilon_{31}. \tag{A18}$$

where λ is the Lamé coefficient, G (also denoted by μ) is the shear modulus of elasticity and δ_{ij} is the Konnecker symbol.

The following relationships between the elastic constants will result:

$$\begin{aligned} C_{11} = C_{22} = C_{33} = \lambda + 2G = \lambda + 2\mu = \tfrac{E(1-\nu)}{(1+\nu)(1-2\nu)}\ ; \\ C_{12} = C_{23} = C_{31} = \lambda = \tfrac{E\nu}{(1+\nu)(1-2\nu)}\ ; \\ C_{44} = C_{55} = C_{66} = G = \mu = \tfrac{E}{2(1+\nu)} = \tfrac{C_{11}-C_{12}}{2}\ . \end{aligned} \tag{A19}$$

If we calculate the ratio:

$$\frac{C_{11}}{C_{12}} = \frac{1-\nu}{\nu}, \tag{A20}$$

it obtains

$$\nu = \frac{C_{12}}{C_{11} + C_{12}};\ \ E = \frac{(C_{11} + 2C_{12})(C_{11} - C_{12})}{C_{11} + C_{12}}. \tag{A21}$$

and

$$\lambda = C_{12} = \frac{E\nu}{(1+\nu)(1-2\nu)}\ ;\ \mu = C_{66} = \frac{E}{2(1+\nu)}. \tag{A22}$$

These relations can be written in an alternative form:

$$\nu = \frac{\lambda}{2(\lambda+\mu)}\ ;\ E = \frac{\mu(3\lambda+2\mu)}{\lambda+\mu}. \tag{A23}$$

The bulk modulus for a two-dimensional body can be expressed as follows:

$$K_{23} = \frac{1}{2}(C_{22} + C_{23}) = \frac{1}{2}\frac{E}{(1+\nu)(1-2\nu)} = \lambda + \mu. \tag{A24}$$

The bulk modulus for a three-dimensional body is as follows:

$$K_{23} = \frac{1}{2}(C_{21} + C_{22} + C_{23}) = \frac{1}{3}(3\lambda + 2\mu) = \frac{E}{3(1-2\nu)}. \tag{A25}$$

Appendix A.3.2. Transversely Isotropic Materials

The following relationships may exist between the engineering constants used in technology and the coefficients of the constitutive equations:

- Bulk modulus:

$$K_{23} = \frac{1}{2}(C_{22} + C_{23}). \tag{A26}$$

- Shear modulus of elasticity:

$$G_{23} = \frac{C_{22} - C_{23}}{2} = C_{55} = C_{66}. \tag{A27}$$

- Shear elastic moduli, perpendicular to the x_2x_3 plane:

$$G_{12} = G_{13} = G_1 = C_{44}. \tag{A28}$$

- Longitudinal modulus of elasticity:

$$E_{11} = C_{11} - \frac{2C_{12}^2}{C_{22} + C_{33}} = C_{11} - \frac{C_{12}^2}{C_{22}} = \frac{C_{11}C_{22} - C_{12}^2}{C_{22}}. \tag{A29}$$

- Poisson's ratio for uniaxial loading in the direction of x_1:

$$\nu_{21} = \nu_{31} = \nu_1 = \frac{1}{2}\left(\frac{C_{11} - E_{11}}{K_{23}}\right)^{\frac{1}{2}} = \frac{C_{12}}{(C_{22} + C_{33})} = \frac{C_{12}}{2C_{22}}. \tag{A30}$$

- Longitudinal Young's modulus corresponding to the x_2x_3 plane:

$$E_{22} = E_{33} = \frac{4G_{23}K_{23}}{K_{23} + \psi G_{23}}. \tag{A31}$$

- Poisson's ratio corresponding to the plane x_2x_3:

$$\nu_{23} = \frac{K_{23} - \psi G_{23}}{K_{23} + \psi G_{23}}. \tag{A32}$$

where

$$\psi = 1 + \frac{4K_{23}\nu_1^2}{E_{11}}. \tag{A33}$$

References

1. Hill, R. Theory of Mechanical Properties of Fiber-strengthened Materials: I Elastic Behavior. *J. Mech. Phys. Solids* **1964**, *12*, 199–212.
2. Hill, R. Continuum Micro-Mechanics of Elastoplastic Polycrystals. *J. Mech. Phys. Solids* **1965**, *13*, 89–101. [CrossRef]
3. Ju, J.W.; Yanase, K. Micromechanical effective elastic moduli of continuous fiber-reinforced composites with near-field fiber interactions. *Acta Mech.* **2011**, *216*, 87–103. [CrossRef]
4. Hashin, Z. On Elastic Behavior of Fibre Reinforced Materials of Arbitrary Transverse Phase Geometry. *J. Mech. Phys. Solids* **1965**, *13*, 119–134.
5. Katouzian, M. On the Effect of Temperature on Creep Behavior of Neat and Carbon Fiber Reinorced PEEK and Epoxy A Micromechanical Approach. Ph.D. Thesis, University of Muenchen, Munich, Germany, 1994. Available online: https://www.osti.gov/etdeweb/biblio/557687 (accessed on 20 March 2026).
6. Hashin, Z.; Shtrikman, S. A Variational Approach to the Theory of the Elastic Behavior of Multiphase Materials. *J. Mech. Phys. Solids* **1963**, *11*, 127–140.
7. Hashin, Z.; Rosen, B.W. The Elastic Moduli of Fiber-Reinforced Materials. *J. Appl. Mech.* **1964**, *31*, 223–232. [CrossRef]
8. Katouzian, M.; Vlase, S.; Marin, M.; Pop, N. Temperature Influence on the Creep Behavior of a Carbon Fiber/Polyetheretherketone Composite. *J. Appl. Comput. Mech.* **2026**, *12*, 1–10. [CrossRef]

9. Bendhia, A.; Devries, F.; Metral, S.; Jomaa, M. Experimental and theoretical modelization and calculus of an aramid fiber rubber composite structure. In Proceedings of the 39th International SAMPE Symposium and Exhibition: Moving Forward with 50 Years of Leadership in Advanced Materials, Anaheim, CA, USA, 11–14 April 1994; pp. 1929–1940.
10. Kanakubo, T.; Echizen, S.; Wang, J.; Mu, Y. Pullout Behavior of Bundled Aramid Fiber in Fiber-Reinforced Cementitious Composite. *Materials* **2020**, *13*, 1746. [CrossRef] [PubMed]
11. Sunaga, D.; Koba, T.; Kanakubo, T. Modeling of Bridging Law for Bundled Aramid Fiber-Reinforced Cementitious Composite and its Adaptability in Crack Width Evaluation. *Materials* **2021**, *14*, 179. [CrossRef] [PubMed]
12. Venetis, J.; Sideridis, E. A lower bound of longitudinal elastic modulus for three-phase fibrous composites. *Math. Mech. Solids* **2019**, *24*, 72–84.
13. Yang, G.; Guo, H.W.; Xiao, H.; Liu, R.Q.; Shi, C. Shear-driving Force and Critical She Angle Analysis of Kevlar/Carbon Fiber Hybrid Composite Skins for a She Variable-sweep Wing Based on the Classical Plate Theory. *Appl. Compos. Mater.* **2022**, *29*, 1871–1887.
14. Spânu, P.; Iliescu, M. Mathematical Model of Temperature in Milling Glass Fiber Reinforced Polymeric Composites. *UPB Sci. Bull. Ser.* **2008**, *70*, 63–72.
15. Risicato, J.V.; Legrand, X. Genetic Algorithm Used to Optimize Fiber Steering in Composite Laminates. Recent Advances in Textile Composites. In Proceedings of the 10th International Conference on Textile Composites (TEXCOMP 10), Lille, France, 26–28 October 2010; pp. 482–489.
16. Iliescu, N.; Hadar, A.; Pastrama, S.D. Combined Researches for Validation of a New Finite Element for Modelling Fiber Reinforced Laminated Composite Plates. *Mater. Plast.* **2009**, *46*, 91–94.
17. Grimaldi, A.; Luciano, R. Tensile stiffness and strength of fiber-reinforced concrete. *J. Mech. Phys. Solids* **2000**, *48*, 1987–2008. [CrossRef]
18. Bolcu, D.; Ursache, M.; Rizescu, S.; Degeratu, S.; Bîzdoaca, N.G.; Stanescu, M.M. The utilization of elasticity matrix spectral decomposition in calculating the elastic properties of a composite bhaving transverse isotropy. *Univ. Politech. Buchar. Sci. Bull.-Ser. A-Appl. Math. Phys.* **2011**, *73*, 177–188.
19. Oliver-Ortega, H.; Llop, M.F.; Espinach, F.X.; Tarrés, Q.; Ardanuy, M.; Mutjé, P. Study of the flexural modulus of lignocellulosic fibers reinforced bio-based polyamide11 green composites. *Compos. Part B-Eng.* **2018**, *152*, 126–132. [CrossRef]
20. Faal, R.T.; Sourki, R.; Crawford, B.; Vaziri, R.; Milani, A.S. Using fractional derivatives for improved viscoelastic modeling of textile composites. Part II: Fabric under different temperatures. *Compos. Struct.* **2020**, *248*, 112494. [CrossRef]
21. Xiang, G.J.; Yin, D.S.; Meng, R.F.; Lu, S.Y. Creep model for natural fiber polymer composites (NFPCs) based on variable order fractional derivatives: Simulation and parameter study. *J. Appl. Polym. Sci.* **2020**, *137*, 48796.
22. Lachenani, A.; Bentchikou, M.; Boumahdi, M.; Hanini, S.; Laidi, M. Drying Process of Cement Mort Composites Reinforced with Cellulosic Fibres: Experiment and Mathematical Modelling. *Kem. Ind. Časopis Kemičara I Kem. Inženjera Hrvat.* **2022**, *71*, 675–684.
23. Zienkiewicz, O.C.; Taylor, R.L.; Zhu, J.Z. *The Finite Element Method: Its Basis and Fundamentals*; Elsevier: Amsterdam, The Netherlands, 2013.
24. Reddy, J.N. *Mechanics of Laminated Composite Plates and Shells*; CRC Press: Boca Raton, FL, USA, 2004.
25. Daniel, I.M.; Ishai, O. *Engineering Mechanics of Composite Materials*; Oxford University Press: Oxford, UK, 2006.
26. Hashin, Z. Failure Criteria for Unidirectional Fiber Composites. *J. Appl. Mech.* **1980**, *47*, 329–334. [CrossRef]
27. Puck, A.; Schürmann, H. Failure Analysis of FRP Laminates by Means of Physically Based Phenomenological Models. *Compos. Sci. Technol.* **2002**, *62*, 1633–1662. [CrossRef]
28. Ansari, M.N.M.; Shanks, R.A. Cellulose Fiber and Nano-Fiber Composites based on Castor Oil-Polyurethane Matrix. In Proceedings of the NSTI Nanotechnology Conference and Expo: Bio Sensors, Instruments, Medical, Environment and Energy, Boston, MA, USA, 13–16 June 2011; 3, pp. 179–182.
29. Mesa, M.C.; Oliete, P.B.; Larrea, A.; Orera, V.M. Directionally Solidified Al_2O_3-$Er_3Al_5O_{12}$-ZrO_2 Eutectic Ceramics with Interpenetrating or Nanofibrill Microstructure: Residual Stress Analysis. *J. Am. Ceram. Soc.* **2012**, *95*, 1138–1146.
30. Skandani, A.A.; Al-Haik, M. Viscoplastic characterization and modeling of hybrid carbon fiber/carbon nanotubes reinforced composites. *Compos. Part B-Eng.* **2016**, *99*, 63–74. [CrossRef]
31. Svoboda, M.; Pahutova, M.; Kucharova, K.; Sklenicka, V.; Kainer, K.U. Microstructure and creep behaviour of magnesium hybrid composites. *Mater. Sci. Eng. A* **2007**, *462*, 220–224. [CrossRef]
32. Skandani, A.A.; Boroujeni, A.Y.; Al-Haik, M. Viscoelastic behavior of epoxy/carbon fiber/Zno nano-rods hybrid composites. *Polym. Compos.* **2015**, *36*, 1967–1972.
33. Haj-Ali, R.M.; Muliana, A.H. A multi-scale constitutive formulation for the nonlinear viscoelastic analysis of laminated composite materials and structures. *Int. J. Solids Struct.* **2004**, *41*, 3461–3490. [CrossRef]
34. Terada, K.; Hirayama, N.; Yamamoto, K.; Kato, J.; Kyoya, T.; Matsubara, S.; Arakawa, Y.; Ueno, Y.; Miyanaga, N. Applicability of micro-macro decoupling scheme to two-scale analysis of fiber-reinforced plastics. *Adv. Compos. Mater.* **2014**, *23*, 421–450.

35. Muliana, A.H.; Haj-Ali, R. A multi-scale framework for layered composites with thermo-rheologically complex behaviors. *Int. J. Solids Struct.* **2008**, *45*, 2937–2963.
36. Wang, S.; Stratford, T.; Reynolds, T.P.S. Line creep of bonded FRP-strengthened metallic structures at warm service temperatures. *Constr. Build. Mater.* **2021**, *283*, 122699.
37. Upadhyaya, P.; Singh, S.; Roy, S. A mechanism-based multi-scale model for predicting thermo-oxidative degradation in high temperature polymer matrix composites. *Compos. Sci. Technol.* **2011**, *71*, 1309–1315.
38. Chen, K.F.; Yang, H.; Wang, A.; Tang, L.S.; Zha, X.; Iita, N.S.; Zhang, H.; Li, Z.X.; Wang, X.Y.; Yang, W.; et al. Smart Driving Hardware Augmentation by Flexible Piezoresistive Sensor Matrices with Grafted-on Anticreep Composites. *Adv. Sci.* **2024**, *12*, e2408313.
39. Song, T.Y.; Xu, M.X.; Weng, Y.J.; Zhang, W.; Shi, Y.Q.; Li, X.; Zhang, Q.; Song, T.Y.; Xu, M.X. Silkworm-Shaped MoS_2 Growing on Graphene Foam for Highly Sensitive and Flexible Strain Sensor with Full-Scale Human Motion Detection Ability. *Adv. Mater. Technol.* **2024**, *10*, 1621.
40. Zhang, B.; Shi, D.Q.; Liu, C.Q.; Hao, W.Q.; Yang, X.G. Physics-informed machine learning with high-throughput design module for evaluating rupture life and guiding design of oxide/oxide ceramic matrix composites. *Ceram. Int.* **2023**, *49*, 34945–34957.
41. Kubo, A.; Umeno, Y. Machine-Learning-Based Atomistic Model Analysis on High-Temperature Compressive Creep Properties of Amorphous Silicon Carbide. *Materials* **2021**, *14*, 1597. [PubMed]
42. Kumar, R.; Banga, H.K.; Kumar, R.; Singh, S.; Scutaru, M.L.; Pruncu, C.I. Ergonomic evaluation of workstation design using taguchi experimental approach: A case of an automotive industry. *Int. J. Interact. Des. Manuf.-IJIDEM* **2021**, *15*, 481–498. [CrossRef]
43. Yang, J.Y.; Kang, G.Z.; Liu, Y.J.; Chen, K.J.; Kan, Q.H. Life prediction for rate-dependent low-cycle fatigue of PA6 polymer considering ratchetting: Semi-empirical model and neural network based approach. *Int. J. Fatigue* **2020**, *136*, 105619.
44. Gheorghe, V.; Scutaru, M.L.; Ungureanu, V.B.; Chircan, E.; Ulea, M. New Design of Composite Structures Used in Automotive Engineering. *Symmetry* **2021**, *13*, 383. [CrossRef]
45. Guedes, R.M. Time-dependent failure criteria for polymer matrix composites: A review. *J. Reinf. Plast. Compos.* **2010**, *29*, 3041–3047. [CrossRef]
46. Evans, A.G.; Zok, F.W. The physics and mechanics of brittle matrix composites. *Solid State Phys.–Adv. Res. Appl.* **1996**, *47*, 177–286.
47. Pulngern, T.; Kaewkalya, P.; Rosarpitak, V.; Sombatsompop, N. Experimental and Computational Investigations of Creep Responses of Wood/PVC Composite Members. *Int. Polym. Process.* **2014**, *29*, 307–316. [CrossRef]
48. Li, B.; Liu, Z.D.; Wang, S. An Experimental Study on Creep Damage of In-Situ TIC-Based Composites. *Adv. Sci. Lett.* **2011**, *4*, 1244–1248.
49. Wang, G.Y.; Li, H.L.; Li, Y.Q. Experimental research on creep properties of composite geomembrane. *Rock Soil Mech.* **2009**, *30*, 1599–1603.
50. Berardi, V.P.; Perrella, M.; Armentani, E.; Cricrì, G. Experimental investigation and numerical modeling of creep response of glass fiber reinforced polymer composites. *Fatigue Fract. Eng. Mater. Struct.* **2021**, *44*, 1085–1095. [CrossRef]
51. Morscher, G.N. Stress-Environmental Effects on Fiber-Reinforced SiC-Based Composites. *Ceram. Matrix Compos. Mater. Model. Technol.* **2014**, 334–352. [CrossRef]
52. Ruggles-Wrenn, M.B. Environmental Effects on Oxide/Oxide Composites. *Ceram. Matrix Compos. Mater. Model. Technol.* **2014**, 295–333. [CrossRef]
53. Raji, M.; Zari, N.; Bouhfid, R.; Qaiss, A.E. Durability of composite materials during hydrothermal and environmental aging. In *Durability and Life Prediction in Biocomposites, Fiber-Reinforced Composites and Hybrid Composites*; Woodhead Publishing: Cambridge, UK, 2019; pp. 83–119. [CrossRef]
54. Barreira-Pinto, R.; Carneiro, R.; Miranda, M.; Guedes, R.M. Polymer-Matrix Composites: Characterising the Impact of Environmental Factors on Their Lifetime. *Materials* **2023**, *16*, 3913. [CrossRef] [PubMed]
55. Miller, S.A.; Lepech, M.D.; Billington, S.L. Evaluation of Functional Units Including Time-Dependent Properties for Environmental Impact Modeling of Biobased Composites. *J. Biobased Mater. Bioenergy* **2013**, *7*, 588–599. [CrossRef]
56. Hiroshima, N.; Hatta, H.; Nagura, Y.; Koyama, M.; Sakai, T.; Kogo, Y. Spin test of three-dimensional composite rotor using polymer ring as a connection device for high-speed flywheel. *Mech. Eng. J.* **2016**, *3*, 16–00261.
57. Chen, Y.F.; Setiawan, L.; Chou, S.R.; Hu, X.; Wang, R. Identification of safe and stable operation conditions for pressure retarded osmosis with high performance hollow fiber membrane. *J. Membr. Sci.* **2016**, *503*, 90–100. [CrossRef]
58. Manu, K.M.S.; Raag, L.A.; Rajan, T.P.D.; Gupta, M.; Pai, B.C. Liquid Metal Infiltration Processing of Metallic Composites: A Critical Review. *Metall. Mater. Trans. B* **2016**, *47*, 2799–2819. [CrossRef]
59. Tanks, J.D.; Rader, K.E.; Sharp, S.R. Accelerated Creep Testing of CFRP with the Stepped Isostress Method. Annual Conference and Exposition of the Society-for-Experimental-Mechanics on Experimental and Applied Mechanics. *Mech. Compos. Multifunct. Mater.* **2016**, *7*, 397–403. [CrossRef]

60. Dasappa, P.; Lee-Sullivan, P.; Xiao, X.R. Development of viscoplastic strains during creep in continuous fiber GMT composites. *Compos. Part B-Eng.* **2010**, *41*, 48–57.
61. Yang, T.C.; Wu, T.L.; Hung, K.C.; Chen, Y.L.; Wu, J.H. Mechanical properties and extended creep behavior of bamboo fiber reinforced recycled poly(lactic acid) composites using the time-temperature superposition principle. *Constr. Build. Mater.* **2015**, *93*, 558–563.
62. Bozorg-Haddad, A.; Iskander, M. Comparison of Accelerated Compressive Creep Behavior of Virgin HDPE Using Thermal and Energy Approaches. *J. Mater. Eng. Perform.* **2011**, *20*, 1219–1229.
63. Scott, D.W.; Lai, J.S.; Zureick, A.H. CREEP-BEHAVIOR OF FIBER-REINFORCED POLYMERIC COMPOSITES-A Review of the Technical Literature. *J. Reinf. Plast. Compos.* **1995**, *14*, 588–617.
64. Papanicolaou, G.C.; Zaoutsos, S.P. Viscoelastic constitutive modeling of creep and stress relaxation in polymers and polymer matrix composites. In *Creep and Fatigue in Polymer Matrix Composites*; Woodhead Publishing: Cambridge, UK, 2011; pp. 3–47.
65. Akshantala, N.V.; Brinson, L.C. A damage evolution model for viscoelastic composite laminates. *J. Compos. Technol. Res.* **2001**, *23*, 3–14. [CrossRef]
66. Drygaś, P.; Gluzman, S.; Mityushev, V.; Nawalaniec, W. *Applied Analysis of Composite Media*; Elsevier: Amsterdam, The Netherlands, 2020.
67. Guedes, R.M. Cumulative creep damage for unidirectional composites under step loading. *Mech. Time-Depend. Mater.* **2012**, *16*, 381–396. [CrossRef]
68. Lim, T.C. Micromechanical Models for Auxetic Materials. In *Auxetic Materials and Structures*; Springer: Singapore, 2014; pp. 45–105.
69. Ouardi, A.; Boukamel, A.; Damil, N. Towards a macro-chain polymer model using a micromechanical approach. In *12th European Conference on Constitutive Models for Rubber (Eccmr), Constitutive Models for Rubber Xii*; CRC Press: Boca Raton, FL, USA, 2022; pp. 112–117.
70. Xu, Z.C.; Shao, X.R.; Huang, Q.B. A micromechanical model of multi-scale nano-reinforced composites. *Polym. Test.* **2023**, *125*, 108121.
71. Ivancevic, D.; Smojver, I. Explicit multiscale modelling of impact damage on laminated composites-Part I: Validation of the micromechanical model. *Compos. Struct.* **2016**, *145*, 248–258.
72. Kim, B.R.; Lee, H.K. An RVE-based micromechanical analysis of fiber-reinforced composites considering fiber size dependency. *Compos. Struct.* **2009**, *90*, 418–427.
73. Katouzian, M.; Vlase, S.; Marin, M.; Scutaru, M.L. Modeling Study of the Creep Behavior of Carbon-Fiber-Reinforced Composites: A Review. *Polymers* **2023**, *15*, 194.
74. Ríos, A.; Martín-Meizoso, A. Micromechanical Model of Interface Between Fibre and Matrix of Metal Matrix Composite Reinforced with Continuous Fibre. *Adv. Mater. Res.* **2008**, *59*, 158–163. [CrossRef]
75. Jiang, W.G.; Wu, Z.K.; Qin, Q.H. A simplified micromechanical model for predicting effective mechanical behaviors of continuous bidirectional-fiber-reinforced composites. *Mech. Adv. Mater. Struct.* **2017**, *24*, 1292–1299.
76. Tabiei, A.; Chen, Q. Micromechanics based composite material model for crashworthiness explicit finite element simulation. *J. Thermoplast. Compos. Mater.* **2001**, *14*, 264–289. [CrossRef]
77. Hadid, L.; Bouafia, F.; Hayat, S.S. Finite element analysis of the interface defect in ceramic-metal assemblies: Alumina-Silver. *Fract. Struct. Integr.* **2020**, *14*, 1–12. [CrossRef]
78. Li, C.Y.; Wang, R. Finite Element Analysis Technique and Its Application in Numerical Simulation of Knitted Fabric. *Adv. Mater. Res.* **2011**, *201–203*, 2567–2570. [CrossRef]
79. Zhao, C.F.; Yin, Z.Y.; Hicher, P.Y. Integrating a micromechanical model for multiscale analyses. *Int. J. Numer. Methods Eng.* **2018**, *114*, 105–127.
80. Kumar, R.; Patil, H.S.; Lal, A. Hygrothermoelastic free vibration response of laminated composite plates resting on elastic foundations with random system properties: Micromechanical model. *J. Thermoplast. Compos. Mater.* **2013**, *26*, 573–604.
81. Chen, X.H.; Mai, Y.W. Micromechanical modelling of deformation mechanisms for rubber-toughened polymers. *Key Eng. Mater.* **1997**, *145-149*, 233–242. [CrossRef]
82. Yang, Q.S.; Xu, F. Effective hyperelastic behaviour of fiber reinforced polymer composite materials. *Key Eng. Mater.* **2007**, *334-335*, 473–476. [CrossRef]
83. Rhim, J.S.; Kim, J.H. Micromechanical RVE model application for generalization of smart composite laminate structures with thermoelastic characteristics. *Mater. Res. Express* **2018**, *6*, 015704. [CrossRef]
84. Cheng, Y.; Cheng, H.; Liu, W.K. A sequential homogenization of multi-coated micromechanical model for functionally graded interphase composites. *Comput. Mech.* **2019**, *64*, 1321–1337. [CrossRef]
85. Scutaru, M.L.; Teodorescu-Draghicescu, H.; Vlase, S.; Marin, M. Advanced HDPE with increased stiffness used for water supply networks. *J. Optoelectron. Adv. Mater.* **2015**, *17*, 484–488.
86. Teodorescu-Draghicescu, H.; Vlase, S.; Calin, M.R. Hysteresis effect in a three-phase polymer matrix composite subjected to static cyclic loadings. *Optoelectron. Adv. Mater.-Rapid Commun.* **2011**, *5*, 273–277.

87. Pintelon, R.; Guillaume, P.; Vanlanduit, S.; De Belder, K.; Rolain, Y. Identification of Young's modulus from broadband modal analysis experiments. *Mech. Syst. Signal Process.* **2004**, *18*, 699–726.
88. Pickering, K.L.; Efendy, M.G.A.; Le, T.M. A review of recent developments in natural fibre composites and their mechanical performance. *Compos. PART A-Appl. Sci. Manuf.* **2016**, *83*, 98–112. [CrossRef]
89. Zangenberg, J.; Jacobsen, T.K.; Ostergaard, R.; Koefoed, M. Material Design and Reliability of Advanced Compoasite Materials. In Proceedings of the 20th International Conference on Composite Materials (ICCM), Copenhagen, Denmark, 19–24 July 2015.
90. Coleman, J.N.; Khan, U.; Blau, W.J.; Gun'ko, Y.K. Small but strong: A review of the mechanical properties of carbon nanotube-polymer composites. *CARBON* **2006**, *44*, 1624–1652.
91. Hasani, S.; Aghamirzaei, M.; Marzbanrad, J. Investigation of Noise Reduction in Vehicle Floor Panels Through Damping Pads: Implications for Human Hearing and Noise Exposure Levels. *Rom. J. Acoust. Vib.* **2025**, *22*, 14–22.
92. Valdiviezo-Mijangos, O.C.; Rodríguez-Ramos, R.; Padilla-Longoria, P. Thermoelastic bounds and self-consistent estimation for the overall properties of composites. *Mech. Res. Commun.* **2020**, *107*, 103555. [CrossRef]
93. Pérez-Fernández, L.D.; Bravo-Castillero, J.; Sabina, F.J. Estimation of very narrow bounds to the behavior of nonlineincompressible elastic composites. *Arch. Appl. Mech.* **2007**, *77*, 229–239.
94. Ronold, K.O.; Echtermeyer, A.T. Using Tolerance Bounds for Estimation of Characteristic Fatigue Curves for Composites with Confidence. *Safety* **2022**, *8*, 1.
95. Quang, H.L. Estimations and bounds of the effective conductivity of composites with anisotropic inclusions and general imperfect interfaces. *Int. J. Heat Mass Transf.* **2016**, *99*, 327–343. [CrossRef]
96. Buryachenko, V.A. Effective field hypothesis in Hashin-Shtrikman bounds estimations for effective moduli of composites with noncanonical shape of inclusions. *Mech. Mater.* **2018**, *119*, 16–24. [CrossRef]
97. Ostoja-Starzewski, M.; Wang, X. Stochastic finite elements as a bridge between random material microstructure and global response. *Comput. Methods Appl. Mech. Eng.* **1999**, *168*, 35–49. [CrossRef]
98. Serban, A. Failure Estimation of the Composite Laminates in Layup Optimization Using Finite Element Analysis and Deep Learning. *J. Fail. Anal. Prev.* **2020**, *20*, 1199–1211. [CrossRef]
99. Chen, N.; Yu, D.J.; Ma, Z.D. Interval and subinterval homogenization-based method for determining the effective elastic properties of periodic microstructure with interval parameters. *Int. J. Solids Struct.* **2017**, *106*, 174–182. [CrossRef]
100. Most, J.; Stegmair, D.; Petry, D. Error estimation between simple, closed-form analytical formulae and full-scale FEM for interlaminstress prediction in curved laminates. *Compos. Struct.* **2015**, *131*, 72–81.
101. You, J.H. Triple-scale failure estimation for a composite-reinforced structure based on integrated modeling approaches. Part 1: Microscopic scale analysis. *Workshop MatModels. Eng. Fract. Mech.* **2009**, *76*, 1425–1436. [CrossRef]
102. Schapery, R. On the Characterization of NonlineViscoelastic Materials. *Polym. Eng. Sci.* **1969**, *9*, 295–310. [CrossRef]
103. Liu, X.Y.; Wu, W.; Liang, N.G. Regularity of strain distribution in short-fiber/whisker reinforced composites. *Mater. Sci. Res. Int.* **2002**, *8*, 219–224.
104. Rossoll, A.; Moser, B.; Mortensen, A. Longitudinal deformation of fibre reinforced metals: Influence of fibre distribution on stiffness and flow stress. *Mech. Mater.* **2005**, *37*, 1–17. [CrossRef]
105. Dong, K.; Liu, K.; Sun, B.Z. Experimental and numerical analyses on the thermal conductive behaviors of carbon fiber/epoxy plain woven composites. *Int. J. Heat Mass Transf.* **2016**, *102*, 501–517. [CrossRef]
106. Tian, W.L.; Qi, L.H.; Zhou, J.M. Numerical evaluation on mechanical properties of short-fiber-reinforced metal matrix composites: Two-step mean-field homogenization procedure. *Compos. Struct.* **2016**, *139*, 96–103. [CrossRef]
107. Chen, Q.; Zhu, H.H.; Yan, Z.G.; Ju, J.W.; Jiang, Z.W.; Wang, Y.Q. A multiphase micromechanical model for hybrid fiber reinforced concrete considering the aggregate and ITZ effects. *Constr. Build. Mater.* **2016**, *114*, 839–850. [CrossRef]
108. Wada, A.; Fukuda, H. Approximate upper and lower bounds for the strength of unidirectional composites. *Compos. Sci. Technol.* **1999**, *59*, 89–95. [CrossRef]
109. Wan, L.; Ismail, Y.; Zhu, C.; Zhu, P.; Sheng, Y.; Liu, J.; Yang, D.M. Computational micromechanics-based prediction of the failure of unidirectional composite lamina subjected to transverse and in-plane shestress states. *J. Compos. Mater.* **2020**, *54*, 3637–3654. [CrossRef]
110. Hara, E.; Yokozeki, T.; Hatta, H.; Iwahori, Y.; Ishikawa, T. Comparison of out-of-plane tensile moduli of CFRP laminates obtained by 3-point bending and direct loading tests. *Compos. Part A-Appl. Sci. Manuf.* **2014**, *67*, 77–85. [CrossRef]
111. Lavergne, F.; Sab, K.; Sanahuja, J.; Bomert, M.; Toulemonde, C. Estimation of creep strain and creep failure of a glass reinforced plastic by semi-analytical methods and 3D numerical simulations. *Mech. Mater.* **2015**, *89*, 130–150. [CrossRef]
112. Schjodt-Thomsen, J.; Pyrz, R. Overall creep modelling of short fibre reinforced composites with weakened interfaces and complex fibre orientation distributions. *Mech. Mater.* **2000**, *32*, 349–359. [CrossRef]
113. Nguyen, B.N.; Kunc, V.; Bapanapalli, S.K. Creep Modeling for Injection-Molded Long-Fiber Thermoplastics. In Proceedings of the ASME International Mechanical Engineering Congress and Exposition, IMECE 2008: Mechanics of Solids, Structures and Fluids, Boston, MA, USA, 31 October–6 November 2008; Volume 12, pp. 511–516.

114. Sakaue, K.; Ochiai, M.; Endo, S.; Takaoka, H. Viscoelastic characteristics of short fiber reinforced polybutylene terephthalate. *Mech. Time-Depend. Mater.* **2020**, *24*, 317–328.
115. Dutra, V.F.P.; Maghous, S.; Campos, A.; Pacheco, A.R. A micromechanical approach to elastic and viscoelastic properties of fiber reinforced concrete. *Cem. Concr. Res.* **2010**, *40*, 460–472. [CrossRef]
116. Li, D.; Hu, G.K. Effective viscoelastic behavior of particulate polymer composites at finite concentration. *Appl. Math. Mech.-Engl. Ed.* **2007**, *28*, 297–307. [CrossRef]
117. You, H.; Lim, H.J.; Yun, G.J. A micromechanics-based time-domain viscoelastic constitutive model for particulate composites: Theory and experimental validation. *Adv. Aircr. Spacecr. Sci.* **2022**, *9*, 217–242.
118. Schjodt-Thomsen, J.; Pyrz, R. Elastic and creep behaviour of short-fibre composites with weakened interfaces. *Key Eng. Mater.* **2001**, *221–222*, 267–280. [CrossRef]
119. He, L.H.; Lim, C.W. Time-dependent interfacial sliding in fiber composites under longitudinal shear. *Compos. Sci. Technol.* **2001**, *61*, 579–584. [CrossRef]
120. Jones, R.M. *Mechanics of Composite Materials*; CRC Press: Boca Raton, FL, USA, 1998.
121. Wang, Y.M.; Weng, G.J. Transient Creep Strain of a Fiber-Reinforced Metal-Matrix Composite under Transverse Loading. *J. Eng. Mater. Technol.-Trans. ASME* **1992**, *114*, 237–244.
122. Shajari, A.R.; Ghajar, R.; Shokrieh, M.M. Multiscale modeling of the viscoelastic properties of CNT/polymer nanocomposites, using complex and time-dependent homogenizations. *Comput. Mater. Sci.* **2018**, *142*, 395–409. [CrossRef]
123. Pan, Y.H.; Zhong, Z. Micromechanical modeling of the wood cell wall considering moisture absorption. *Compos. Part B-Eng.* **2016**, *91*, 27–35. [CrossRef]
124. Spilker, K.; Lebensohn, R.A.; Jacobsen, G.; Capolungo, L. A mean field homogenization model for the mechanical response of ceramic matrix composites. *Compos. Struct.* **2025**, *352*, 118630.
125. Mercier, S.; Molinari, A.; Berbenni, S.; Berveiller, M. Comparison of different homogenization approaches for elastic-viscoplastic materials. *Model. Simul. Mater. Sci. Eng.* **2012**, *20*, 024004.
126. Chen, Q.; Wang, G.N.; Chen, X.; Geng, J. Finite-volume homogenization of elastic/viscoelastic periodic materials. *Compos. Struct.* **2017**, *182*, 457–470.
127. Wang, X. Nonuniform Interfacial Slip in Fibrous Composites. *J. Mech. Mater. Struct.* **2009**, *4*, 107–119. [CrossRef]
128. Xu, W.; Nobutada, O. A Homogenization Theory for Time-Dependent Deformation of Composites with Periodic Internal Structures. *JSME Int. J. Ser. A Solid Mech. Mater. Eng.* **1998**, *41*, 309–317. [CrossRef]
129. Duvaut, G. Homogénéisation des plaques à structure périodique en théorie non linéaire de Von Karman. *Lect. Notes Math.* **1977**, *665*, 56–69.
130. Sanchez-Palencia, E. Homogenization method for the study of composite media. In *Asymptotic Analysis II Lecture Notes in Mathematics*; Verhulst, F., Ed.; Springer: Berlin/Heidelberg, Germany, 1983; Volume 985.
131. Bledzki, A.K.; Gassan, J. Composites reinforced with cellulose based fibres. *Prog. Polym. Sci.* **1999**, *24*, 221–274. [CrossRef]
132. Bugaru, M.; Vasile, O. Modeling and Analysis of FBV Movements for Automotive Driveshafts in the PPR Region. *Appl. Sci.* **2022**, *12*, 3237. [CrossRef]
133. Kondo, K.; Takiguchi, R. Finite element analysis of creep in unidirectional composites based on homogenization theory. *Adv. Compos. Mater.* **2002**, *11*, 31–39. [CrossRef]
134. Su, X.L.; Wu, Y.; Jia, M.K.; Yao, L.Q.; Xu, W.X. Creep evaluation for fiber- reinforced composites with hybrid fibers: From quantifying fiber anchorage effect to homogenization model. *J. Build. Eng.* **2024**, *98*, 111204. [CrossRef]
135. Lavergne, F.; Sab, K.; Sanahuja, J.; Bornert, M.; Toulemonde, C. An approximate multiscale model for aging viscoelastic materials exhibiting time-dependent Poisson's ratio. *Cem. Cincrete Res.* **2016**, *86*, 42–54.
136. Mahmoodi, M.J.; Hassanzadeh-Aghdam, M.K.; Safi, M. Effects of nano-sized silica particles on the off-axis creep performance of unidirectional fiber-reinforced polymer hybrid composite. *J. Compos. Mater.* **2021**, *55*, 1575–1589.
137. Iacovescu, S.A.; Polidor-Paul Bratu, P.-P.; Nicolae–Doru Stanescu, N.D. Influence of Different Mechanical Parameters on the Dynamics of a Medical Device. *Rom. J. Acoust. Vib.* **2025**, *22*, 39–45.
138. Pedoto, G.; Grandidier, J.C.; Gigliotti, M.; Vinet, A. Assessment and simulation of the thermomechanical tensile and creep behavior of C/PEKK composites for aircraft applications above the glass transition temperature. *Compos. Struct.* **2023**, *318*, 117069. [CrossRef]
139. Marr, J.; Zartmann, L.; Reinel-Bitzer, D.; Andrä, H.; Müller, R. Multiscale optimization of the viscoelastic behavior of short fiber reinforced composites. *Int. J. Mech. Mater. Des.* **2023**, *19*, 501–519. [CrossRef]
140. Rodríguez-Ramos, R.; Otero, J.A.; Cruz-González, O.L.; Guinovart-Díaz, R.; Bravo-Castillero, J.; Sabina, F.J.; Padilla, P.; Lebon, F.; Sevostianov, I. Computation of the relaxation effective moduli for fibrous viscoelastic composites using the asymptotic homogenization method. *Int. J. Solids Struct.* **2020**, *190*, 281–290. [CrossRef]
141. Escarpini, R.D.; Marques, S.P.C. A Model for Homogenization of Line Viscoelastic Periodic Composite Materials with Imperfect Interface. *Lat. Am. J. Solids Struct.* **2016**, *13*, 2406–2435. [CrossRef]

142. Birman, V.; Byrd, L.W. Modeling and analysis of functionally graded materials and structures. *Appl. Mech. Rev.* **2007**, *60*, 195–216. [CrossRef]
143. Cheng, C.; Aravas, N. Creep of metal-matrix composites with elastic fibers.1. Continuous aligned fibers. *Int. J. Solids Struct.* **1997**, *34*, 4147–4171.
144. Sosa-Rey, F.; Lingua, A.; Piccirelli, N.; Therriault, D.; Lévesque, M. Thermo-viscoelastic multiscale homogenization of additively manufactured short fiber reinforced polymers from direct microstructure characterization. *Int. J. Solids Struct.* **2023**, *281*, 112421. [CrossRef]
145. Otero, J.A.; Rodríguez-Ramos, R.; Guinovart-Díaz, R.; Cruz-González, O.L.; Sabina, F.J.; Berger, H.; Böhlke, T. Asymptotic and numerical homogenization methods applied to fibrous viscoelastic composites using Prony's series. *Acta Mech.* **2020**, *231*, 2761–2771. [CrossRef]
146. Katouzian, M.; Vlase, S.; Marin, M.; Scutaru, M.L. Calculation of Homogenized Mechanical Coefficients of Fiber-Reinforced Composite Using Finite Element Method. *Materials* **2024**, *17*, 1334. [CrossRef] [PubMed]
147. Castañeda, P.P. Second-order homogenization estimates for nonlinear composites incorporating field fluctuations: I – theory. *Jourbal Mech. Phys. Solids* **2002**, *50*, 737–757. [CrossRef]
148. Köbler, J.; Schneider, M.; Ospald, F.; Andrä, H.; Müller, R. Fiber orientation interpolation for the multiscale analysis of short fiber reinforced composite parts. *Comput. Mech.* **2018**, *61*, 729–750. [CrossRef]
149. Reinaldo, A.; Javier, M.; Pablo, S. Multiscale formulation for saturated porous media preserving the representative volume element size objectivity. *Int. J. Numer. Methods Eng.* **2024**, *125*, e7381.
150. Khoei, A.R.; Saeedmonir, S. Computational homogenization of fully coupled multiphase flow in deformable porous media. *Comput. Methods Appl. Mech. Eng.* **2021**, *376*, 113660. [CrossRef]
151. Saeedmonir, S.; Khoei, A.R. Multiscale modeling of coupled thermo-hydro-mechanical analysis of heterogeneous porous media. *Comput. Methods Appl. Mech. Eng.* **2022**, *391*, 114518.
152. Pei, Q.X.; Li, F.; Fei, Z.H.; Lian, H.J.; Yuan, X.H. A DFE2-SPCE Method for Multiscale Parametric Analysis of Heterogenous Piezoelectric Materials and Structures. *CMC-Comput. Mater. Contin.* **2025**, *83*, 79–96. [CrossRef]
153. Dey, A.P.; Welschinger, F.; Schneider, M.; Gajek, S.; Böhlke, T. Rapid inverse calibration of a multiscale model for the viscoplastic and creep behavior of short fiber-reinforced thermoplastics based on Deep Material Networks. *Int. J. Plast.* **2023**, *160*, 103484.
154. Hernandez, Y.; Nicolosi, V.; Lotya, M.; Blighe, F.M.; Sun, Z.Y.; De, S.; McGovern, I.T.; Coleman, J.N. High-yield production of graphene by liquid-phase exfoliation of graphite. *Nat. Nanotechnol.* **2008**, *3*, 563–568. [PubMed]
155. Bourgogne, Q.C.P.; Bouchart, V.; Chevrier, P.; Dinzart, F. On the thermo-visco-elastic behavior of neat and aged PPS composites. *Int. J. Mech. Sci.* **2024**, *284*, 109761.
156. Aboudi, J. Micromechanics-based thermoviscoelastic constitutive equations for rubber-like matrix composites at finite strains. *Int. J. Solids Struct.* **2024**, *41*, 5611–5629.
157. Launay, A.; Maitournam, M.H.; Marco, Y.; Raoult, I. Multiaxial fatigue models for short glass fiber reinforced polyamide-Part I: Nonlinear anisotropic constitutive behavior for cyclic response. *Int. J. Fatigue* **2013**, *47*, 382–389.
158. Klasztorny, M.; Niezgoda, T. Viscoelastic Modeling of RegulCross-Ply Laminates. *Compos. Theory Pract.* **2009**, *9*, 223–227.
159. Fanara, A.; Courard, L.; Collin, F. Numerical FE2 study of chloride ingress in unsaturated recycled aggregates concrete. *Cem. Concr. Res.* **2024**, *186*, 107703.
160. Marinelli, F.; van den Eijnden, A.P.; Collin, F. Modeling of granular solids with computational homogenization: Comparison with Biot's theory. *Finite Elem. Anal. Des.* **2016**, *119*, 45–62.
161. Moës, N.; Cloirec, M.; Remacle, J.F. A computational approach to handle complex microstructure geometries. Workshop on Multiscale Computational Mechanics for Materials and Structures. *Comput. Methods Appl. Mech. Eng.* **2003**, *192*, 3163–3177.
162. Cai, Y.W.; Xu, L.; Cheng, G.D. Novel numerical implementation of asymptotic homogenization method for periodic plate structures. *Int. J. Solids Struct.* **2014**, *51*, 284–292. [CrossRef]
163. Smit, R.J.M.; Brekelmans, W.A.M.; Meijer, H.E.H. Prediction of the mechanical behavior of nonlinear heterogeneous systems by multi-level finite element modeling. *Comput. Methods Appl. Mech. Eng.* **1998**, *155*, 181–192. [CrossRef]
164. Berger, H.; Kari, S.; Bravo-Castillero, J. An analytical and numerical approach for calculating effective material coefficients of piezoelectric fiber composites. *Int. J. Solids Struct.* **2005**, *42*, 5692–5714.
165. Cruz-González, O.L.; Rodríguez-Ramos, R.; Lebon, F. On the effective behavior of viscoelastic composites in three dimensions. *Int. J. Eng. Sci.* **2020**, *157*, 103377. [CrossRef]
166. Schneider, M.; Ospald, F.; Kabel, M. Computational homogenization of elasticity on a staggered grid. *Int. J. Numer. Methods Eng.* **2016**, *105*, 693–720.
167. Kalamkarov, A.L.; Georgiades, A.V.; Ghasemi-Nejhad, M.N. Analytical and numerical techniques to predict carbon nanotubes properties. *Int. J. Solids Struct.* **2006**, *43*, 6832–6854. [CrossRef]
168. Yang, G.; Qi, Y.; Xu, J. A Study on Equivalent Elastic Properties of Crumb Rubber Concrete Based on a Mesoscale Numerical Homogenization Method. *Appl. Sci.* **2026**, *16*, 2936. [CrossRef]

169. Pham, Q.X.; Lee, K. Reduced basis homogenization of thermal and elastic properties for periodic composite materials. *Int. J. Mech. Sci.* **2025**, *304*, 109801.
170. Dastgir, N.; Ansari, R.; Sahmani, S. Finite element analysis of the electro-mechanical behaviors of piezocomposite bimorph energy harvesters under static and dynamic loadings. *Compos. Commun.* **2025**, *59*, 102573. [CrossRef]
171. Huynh, D.B.P.; Belytschko, T. The extended finite element method for fracture in composite materials. *Int. J. Numer. Methods Eng.* **2009**, *77*, 214–239.
172. Shetty, N.; Shahabaz, S.M.; Shetty, S.D. A review on finite element method for machining of composite materials. *Compos. Struct.* **2017**, *176*, 790–802. [CrossRef]
173. Kimyong, C.; Aimmanee, S.; Wechsatol, W. Micromechanics damage analysis in fiber-reinforced composite material using finite element method. *Key Eng. Mater.* **2012**, *525–526*, 541–544. [CrossRef]
174. Cao, L.Q.; Cui, J.Z.; Luo, J.L. Multiscale finite element method for subdivided periodic elastic structures of composite materials. *J. Comput. Math.* **2001**, *19*, 205–212.
175. Lian, Z.Q.; Tang, C.Y.; Chow, C.L. Progressive damage modeling of porous composite materials by multi-scale finite element method. *J. Serbian Soc. Comput. Mech.* **2011**, *5*, 78–88.
176. Hou, T.Y.; Wu, X.H. A multiscale finite element method for elliptic problems in composite materials and porous media. *J. Comput. Phys.* **1997**, *134*, 169–189. [CrossRef]
177. Andrianov, I.; Gluzman, S.; Mityushev, V. (Eds.) *Mechanics and Physics of Structured Media: Asymptotic and Integral Equations Methods of Leonid Filshtinsky*; Academic Press: Cambridge, MA, USA, 2022.
178. Zhai, P.C.; Zhang, Q.J.; Yuan, R.Z. Random microstructure finite element method for effective nonlinear properties of composite materials. *J. Wuhan Univ. Technol.-Mater. Sci. Ed.* **2011**, *15*, 1–6.
179. Ling, D.S.; Yang, Q.D.; Cox, B. An augmented finite element method for modeling arbitrary discontinuities in composite materials. *Int. J. Fract.* **2009**, *156*, 53–73. [CrossRef]
180. Berger, H.; Gabbert, U.; Maugin, G.A. Finite element and asymptotic homogenization methods applied to smart composite materials. *Comput. Mech.* **2003**, *33*, 61–67. [CrossRef]
181. Zhang, W.Y.; Guo, R.; Xu, W. Arbitrary multiphase hybri stress finite element method for composite materials. *Compos. Struct.* **2025**, *358*, 118974.
182. Sun, H.Y.; Di, S.L.; Wu, C.C. Micromechanics of composite materials using multivariable finite element method and homogenization theory. *Int. J. Solids Struct.* **2001**, *38*, 3007–3020. [CrossRef]
183. Alves, G.D.; Evangelista, F.; de Paivab, G.O.F. A generalized finite element interface method for mesh reduction of composite materials simulations. *Lat. Am. J. Solids Struct.* **2022**, *19*, e465. [CrossRef]
184. Chang, C.K.; Bayandor, J. Study on Fracture Simulation of Composite Material Structures by Extended Finite Element Method. *J. Chin. Soc. Mech. Eng.* **2023**, *44*, 371–377.
185. Jeon, Y.J.; Yun, J.H.; Kang, M.S. Analysis of Elastic Properties of Al/PET Isotropic Composite Materials Using Finite Element Method. *Materials* **2022**, *15*, 8007. [CrossRef] [PubMed]
186. Tseng, B.Y.; Chen, Y.W.; Yu, C.H. Optimizing Bioinspired Composite Materials Using Deep Q-Network Reinforcement Learning and Finite Element Methods. *Adv. Eng. Mater.* **2025**, *27*, 2807.
187. Czaplinski, T.; Drygaś, P.; Gluzman, S.; Mityushev, V.; Nawalaniec, W.; Zietek, G. Elastic properties of a unidirectional composite reinforced with a hexagonal array of fibers. *Arch. Mech.* **2018**, *70*, 207–239.
188. Singleton, T.; Saeed, A.; Strawbridge, L.; Khan, Z. Finite Element Analysis of Manufacturing Deformation in Polymer Matrix Composites. *Materials* **2024**, *17*, 2228. [CrossRef] [PubMed]
189. Apsan, M.R.; Mitu, A.M.; Pop, N.; Sireteanu, T.; Maxim, V.M.; Musat, A. Analysis and Numerical Simulation of the Behavior of Composite Materials with Natural Fibers Under Quasi-Static Frictional Contact. *J. Compos. Sci.* **2025**, *9*, 338. [CrossRef]
190. Itu, C.; Scutaru, M.L.; Vlase, S. Elastic Constants of Polymeric Fiber Composite Estimation Using Finite Element Method. *Polymers* **2024**, *16*, 354. [CrossRef] [PubMed]
191. Timoshenko, T. *Strength of Materials, Part 1: Elementary Theory and Problems*, 3rd ed.; CBS Publishers & Distributors Pvt Ltd.: New Delhi, India, 2002.
192. Teodorescu-Draghicescu, H.; Scutaru, M.L.; Grigore, P. New Advanced Sandwich Composite with twill weave carbon and EPS. *J. Optoelectron. Adv. Mater.* **2013**, *15*, 199–203.
193. Bratu, P.; Dobrescu, C.; Nitu, M.C. Dynamic Response Control of LineViscoelastic Materials as Resonant Composite Rheological Models. *Rom. J. Acoust. Vib.* **2023**, *20*, 73–77.
194. Bratu, P.; Nitu, M.C.; Tonciu, O. Effect of Vibration Transmission in the Case of the Vibratory Roller Compactor. *Rom. J. Acoust. Vib.* **2023**, *20*, 67–72.
195. Drygas, P.; Rylko, N. Plane-strain elastic problem for a square array of disks. i. elastic field in a composite with soft inclusions. *J. Appl. Mech. Tech. Phys.* **2024**, *65*, 354–367. [CrossRef]

196. Czapla, R.; Drygaś, P.; Gluzman, S.; Ligocki, T.; Mityushev, V. Computational Strategy for Analyzing Effective Properties of Random Composites-Part II: Elasticity. *Materials* **2025**, *18*, 5041. [PubMed]
197. Bouakba, T.; Zouggar, K.; Guerraiche, K.; Guerraiche, D.; Fiala, H.E.; Harmel, M.W.; Benyettou, M.; Madani, K. Experimental and numerical study of the mechanical response and progressive failure of Hexel IM2-12K/Epocast 50-A1 composite. *J. Compos. Mater.* **2025**, *60*, 1057–1079. [CrossRef]

Disclaimer/Publisher's Note: The statements, opinions and data contained in all publications are solely those of the individual author(s) and contributor(s) and not of MDPI and/or the editor(s). MDPI and/or the editor(s) disclaim responsibility for any injury to people or property resulting from any ideas, methods, instructions or products referred to in the content.